

Non-minimally coupled loop quantum inflation with inverse-volume corrections

Rudranil Roy^a, Giovanni Otalora^a, Joel Saavedra^b, Salvatore Capozziello^{c,d,e}

^a*Departamento de Física, Facultad de Ciencias, Universidad de Tarapacá, Casilla 7-D, Arica, Chile*

^b*Instituto de Física, Pontificia Universidad Católica de Valparaíso, Casilla 4950, Valparaíso, Chile*

^c*Dipartimento di Fisica “E. Pancini”, Università degli Studi di Napoli “Federico II”, Complesso Universitario di Monte Sant’Angelo, Edificio G, Via Cinthia, I-80126, Napoli, Italy*

^d*Istituto Nazionale di Fisica Nucleare (INFN), Sezione di Napoli, Via Cinthia 9, I-80126, Napoli, Italy*

^e*Scuola Superiore Meridionale, Via Mezzocannone 4, I-80134, Napoli, Italy*

Abstract

We study slow-roll inflation driven by a scalar field non-minimally coupled to gravity within the effective framework of Loop Quantum Cosmology (LQC), including inverse-volume corrections. We consider two physically motivated classes of potentials, a Higgs-like quartic potential $V \propto \phi^4$ and string-inspired fractional monomial potentials $V \propto \phi^p$ with $p < 1$. Working at first order in the slow-roll expansion, we derive analytic expressions for the inflationary observables, namely the scalar spectral index n_s , the tensor-to-scalar ratio r , and the running $\alpha_s \equiv dn_s/d \ln k$, and then solve the corrected background dynamics numerically to obtain quantitative predictions. Confronting these results with current observational constraints from Planck 2018 and ACT DR6, we find that the model can lie within the allowed region of the (n_s, r, α_s) parameter space, including a mild preference for slightly larger n_s , as suggested by recent ground-based measurements. We also compute the probability of achieving sufficient slow-roll inflation in this setting. Although effective LQC replaces the initial singularity with a nonsingular quantum bounce, the likelihood of a sufficiently long inflationary phase depends on the pre-inflationary dynamics and on the inflaton potential. Using the canonical Liouville measure on the effective phase space, we determine the fraction of post-bounce trajectories that yield sufficient inflation and find that the non-minimal coupling parameter ξ substantially enlarges the phase-space volume of favorable initial conditions relative to the minimally coupled case, exhibiting an attractor-like enhancement that saturates at large ξ .

1. Introduction

Cosmic inflation has emerged as the leading theoretical framework for describing the earliest stages of the universe Guth (1981); Starobinsky (1980); Linde (1982); Albrecht and Steinhardt (1982). It provides a natural explanation for the observed homogeneity, isotropy, and flatness of the cosmos, while also accounting for the primordial fluctuations imprinted in the cosmic microwave background (CMB) and the large-scale structure of the universe Mukhanov and Chibisov (1981); Bardeen et al. (1983); Akrami et al. (2020); Liddle and Lyth (2000). Numerous inflationary models successfully reproduce current observational constraints, as reviewed in several foundational works Martin et al. (2014); Kallosh and Linde (2025); Gao et al. (2025); Ellis et al. (2025); Kumar et al. (2025). Despite these successes, key conceptual challenges remain, including the sensitivity of inflation to initial conditions Goldwirth and Piran (1990); Brandenberger (2016); Linde (2018); Clough et al. (2017); East et al. (2016) and the need for a consistent ultraviolet (UV) completion that embeds inflation within a fundamental quantum gravitational theory Burgess (2007); Baumann and McAllister (2015).

Loop Quantum Cosmology (LQC), a symmetry-reduced quantization derived from Loop Quantum Gravity Ashtekar (1986, 1987); Rovelli and Smolin (1988, 1990); Rovelli (2004); Thiemann (2007); Ashtekar and Lewandowski (2004); Perez (2013); Gambini and Pullin (2011), offers an appealing avenue for addressing these issues. One of its most notable predictions is the replacement of the big-bang singularity by a quantum bounce, a consequence of the discrete

Email addresses: rudranil.roy@alumnos.uta.cl (Rudranil Roy), giovanni.otalora@academicos.uta.cl (Giovanni Otalora), joel.saavedra@pucv.cl (Joel Saavedra), capozziello@na.infn.it (Salvatore Capozziello)

quantum geometry underlying the theory [Ashtekar and Singh \(2011\)](#); [Ashtekar et al. \(2006\)](#). This modification introduces non-classical phases such as superinflation and alters the effective Friedmann dynamics [Copeland et al. \(2008\)](#); [Bojowald \(2002a\)](#); [Bojowald and Vandersloot \(2003\)](#); [Ashtekar and Sloan \(2011a\)](#). As a result, the pre-inflationary evolution is significantly changed, and the space of initial conditions capable of yielding sufficient slow-roll inflation is reshaped [Ashtekar and Sloan \(2011a,b\)](#). Prior studies have shown that for minimally coupled scalar fields, LQC dynamics generally increase the likelihood of achieving successful inflation, although the degree of enhancement depends on the chosen potential and model details [Ashtekar and Sloan \(2011b\)](#); [Bedić and Vereshchagin \(2019\)](#); [Vereshchagin and Bedić \(2018\)](#).

In the effective description of LQC, quantum geometric effects arise primarily through two distinct mechanisms associated with the underlying discreteness of space. The first, known as holonomy corrections, originates from representing the curvature (field strength) of the Ashtekar-Barbero connection by holonomies around loops of minimal nonzero area. These corrections are responsible for singularity resolution via the “Big Bounce” and provide the dominant modification in the high-curvature (Planck) regime. Extensive studies have already analyzed the probability of inflation, focusing primarily on these corrections [Li and Singh \(2024\)](#); [Barboza et al. \(2020\)](#); [Graef and Ramos \(2018\)](#); [Bedić and Vereshchagin \(2019\)](#); [Ashtekar and Sloan \(2011b\)](#); [Chen and Zhu \(2015\)](#). The second mechanism, inverse volume corrections, arises from the quantization of operators involving inverse powers of the densitized triad (or equivalently the scale factor), which diverge classically but remain finite in LQC. In contrast to holonomy effects, inverse-volume modifications of the effective Hamiltonian and the equations of motion are not strictly confined to the deep Planck regime and may persist into the semi-classical phase [Bojowald \(2007\)](#); [Germani et al. \(2007\)](#). While the effect of holonomy corrections on inflationary probabilities has been intensively investigated, a distinct gap remains regarding the specific impact of inverse volume corrections. Since these modifications may influence the phase-space flow during the onset of slow-roll inflation, in this work, we specifically focus our analysis on filling this gap in the literature.

A theoretically well-motivated extension of inflation is to include a non-minimal coupling between the inflaton and the Ricci scalar, typically written as $\xi\phi^2R$. In quantum field theory in curved spacetime, this operator is generically generated by renormalization and should therefore be included in the effective action, even if it is absent at the classical level [Birrell and Davies \(1982\)](#); [Buchbinder et al. \(1992\)](#). In an effective field theory formulation, it is likewise allowed by the symmetries and appears in the low-energy action with a coefficient that encodes ultraviolet sensitivity and the effects of integrating out heavy degrees of freedom [Baumann and McAllister \(2015\)](#); [Cheung et al. \(2008\)](#). Similar expectations apply in quantum-gravity motivated settings, where radiative and threshold effects typically induce such interactions in the low-energy effective action, as expected in ultraviolet completions such as string theory and higher-dimensional constructions [Baumann and McAllister \(2015\)](#); [Polchinski \(2007\)](#).

The non-minimal coupling has direct dynamical consequences. It makes the effective gravitational coupling field dependent in the Jordan frame and modifies the slow-roll conditions, thereby altering the relation between Lagrangian parameters and inflationary observables. Higgs inflation provides a representative example, since a sizable ξ flattens the potential in the Einstein frame and allows the Higgs field to sustain slow-roll inflation within an economical setting connected to particle physics [Bezrukov and Shaposhnikov \(2009\)](#). More broadly, scalar-tensor theories provide a systematic framework for analyzing these effects and confronting them with observations [De Felice and Tsujikawa \(2010\)](#); [Capozziello and De Laurentis \(2011\)](#); [Clifton et al. \(2012\)](#); [Kobayashi \(2019\)](#); [López et al. \(2021\)](#); [Leyva and Otalora \(2023\)](#).

A recent study confronted inverse-volume corrections in LQC with current data by considering loop quantum inflation driven by a canonical minimally coupled scalar field, with particular emphasis on low-scale spontaneously broken supersymmetric (SB SUSY) and exponential inflationary potentials [Parvizi et al. \(2026\)](#). In this work, we extend that analysis by incorporating inverse-volume corrections together with a non-minimal coupling $\xi\phi^2R$. Working at first order in the slow-roll expansion, we derive analytic expressions for the scalar spectral index n_s , the tensor-to-scalar ratio r , and the running $\alpha_s \equiv dn_s/d\ln k$, and we complement these results with numerical solutions of the corrected background evolution. We confront the resulting predictions with Planck 2018 [Akrami et al. \(2020\)](#) and ACT DR6 constraints [Louis et al. \(2025\)](#); [Calabrese et al. \(2025\)](#). We also compute the probability of obtaining $N \geq N_*$ e-folds after the bounce, defined through the Liouville measure on the effective phase space [Ashtekar and Sloan \(2011b\)](#); [Bedić and Vereshchagin \(2019\)](#); [Bojowald and Kagan \(2006\)](#); [Han \(2019\)](#), and assess how the non-minimal coupling modifies the phase-space volume of initial conditions leading to sufficient inflation.

We consider two classes of potentials. First, we study non-minimally coupled Higgs inflation with a quartic potential in the regime where the symmetry-breaking scale is negligible during inflation [Bezrukov and Shaposhnikov \(2008\)](#). Recent ACT DR6, SPT-3G, and DESI 2024 BAO results favor slightly larger n_s than Planck 2018 [Akrami et al. \(2020\)](#) alone, while maintaining stringent upper bounds on the tensor-to-scalar ratio [Louis et al. \(2025\)](#); [Calabrese et al. \(2025\)](#); [Camphuis et al. \(2025\)](#); [Adame et al. \(2025a,b\)](#). Depending on the dataset combination, this can place tension on plateau-type attractor models, including Starobinsky inflation and the standard Higgs-inflation limit, as reviewed in Ref. [Kallosh and Linde \(2025\)](#). In this context, quantum-corrected ϕ^4 -type modifications of the effective potential, for instance from renormalization-group improved Higgs self-interactions, can bring Higgs inflation into improved agreement with the ACT-DESI preferred region [Gialamas et al. \(2025\)](#); [Yuennan et al. \(2025\)](#); [Maity \(2025\)](#). We examine whether inverse-volume corrections in LQC can provide an additional shift of the predictions toward the region favored by current data.

Second, we analyze string-inspired fractional monomial potentials of the form $V(\phi) \propto \phi^p$, motivated by axion-monodromy and related ultraviolet constructions [Silverstein and Westphal \(2008\)](#); [McAllister et al. \(2010\)](#); [Martin et al. \(2014\)](#). The preference for larger n_s renews interest in these models, particularly for $p < 1$, which can lie within the ACT-DESI preferred region [Kallosh et al. \(2025\)](#); [Maity \(2025\)](#). Together, these two cases allow us to assess how potential shape and non-minimal coupling interplay with inverse-volume corrections in determining both the inflationary predictions and the probability of sufficiently long inflation.

The paper is organized as follows. Section 2 reviews the background dynamics of inflation in generalized non-minimally coupled scalar–tensor theories. Section 3 discusses the construction of the Liouville measure and its quantum-corrected form in LQC. Section 4 analyzes Higgs inflation with non-minimal coupling, while Section 5 extends the discussion to string-inspired fractional monomial potentials. Section 6 presents our conclusions. Throughout, we work in natural units $\hbar = c = 1$, and M_{Pl} denotes the reduced Planck mass.

2. Inflation in a generalized non-minimally coupled gravity

In this section, we briefly review the background dynamics and the linear theory of cosmological perturbations for inflation in a generalized scalar-tensor theory with a non-minimal coupling.

2.1. Cosmological background evolution

We start from the Jordan-frame action

$$S = \int d^4x \sqrt{-g} \left[\frac{U(\phi)}{2\kappa} R - \frac{1}{2} \partial_\mu \phi \partial^\mu \phi - V(\phi) \right], \quad (1)$$

where $\kappa \equiv 1/M_{Pl}^2$.

This action describes a canonical scalar field ϕ with potential $V(\phi)$, non-minimally coupled to gravity through the coupling function $U(\phi)$ [De Felice and Tsujikawa \(2010\)](#); [De Felice et al. \(2011\)](#); [De Felice and Tsujikawa \(2011\)](#); [López et al. \(2021\)](#).

For the background, we assume a spatially flat Friedmann–Lemaître–Robertson–Walker (FLRW) spacetime

$$ds^2 = -dt^2 + a(t)^2 \delta_{ij} dx^i dx^j, \quad (2)$$

where $a(t)$ is the scale factor. Substituting (2) into (1) and discarding total derivatives, one obtains the minisuperspace Lagrangian density [Faraoni and Capozziello \(2011\)](#)

$$\mathcal{L} = a^3 \left[\frac{1}{2} \dot{\phi}^2 - V - \frac{3}{\kappa} (UH^2 + \dot{U}H) \right], \quad (3)$$

where $H \equiv \dot{a}/a$ is the Hubble rate, and $\dot{U} \equiv dU/dt$.

From (3) we define the Hamiltonian density in the standard way,

$$\mathcal{H} \equiv \dot{\phi} \frac{\partial \mathcal{L}}{\partial \dot{\phi}} + \dot{a} \frac{\partial \mathcal{L}}{\partial \dot{a}} - \mathcal{L}, \quad (4)$$

which yields

$$\mathcal{H} = a^3 \left[\frac{1}{2} \dot{\phi}^2 + V - \frac{3}{\kappa} (UH^2 + \dot{U}H) \right]. \quad (5)$$

The Hamiltonian constraint $\mathcal{H} = 0$ in (5) can be written as the first Friedmann equation,

$$H^2 = \frac{\kappa}{3U(\phi)} \left(\frac{1}{2} \dot{\phi}^2 + V(\phi) \right) - H \frac{\dot{U}(\phi)}{U(\phi)}. \quad (6)$$

The second Friedmann equation can also be obtained directly from the mini-superspace Lagrangian by varying it with respect to the scale factor

$$\frac{1}{2} \dot{\phi}^2 - V + \frac{U}{\kappa} \left(\frac{\ddot{a}}{a} + H^2 \right) + \frac{U'}{\kappa} (\dot{\phi} + 2H\phi) = 0. \quad (7)$$

Similarly, the modified Klein-Gordon equation is obtained by varying with respect to ϕ

$$\ddot{\phi} + 3H\dot{\phi} + V' - \frac{3U'}{\kappa} \left(\frac{\ddot{a}}{a} + H^2 \right) = 0, \quad (8)$$

where a prime denotes the derivative with respect to ϕ . The set of field equations (6), (7), and (8) constitutes the full system of cosmological equations for the non-minimally coupled scalar field model. However, only two of these field equations are independent.

To study the inflationary dynamics, we introduce the slow-roll parameters [De Felice and Tsujikawa \(2011\)](#)

$$\begin{aligned} \epsilon &= -\frac{\dot{H}}{H^2}, \quad \delta_\phi = \frac{\ddot{\phi}}{H\dot{\phi}}, \quad \delta_X = \frac{\kappa X}{H^2 U}, \\ \delta_U &= \frac{\dot{U}}{HU}, \quad \delta_{\dot{U}} = \frac{\ddot{U}}{H\dot{U}}, \end{aligned} \quad (9)$$

where $X = -\partial_\mu \phi \partial^\mu \phi / 2$. During inflation, these parameters are assumed to be small, which defines the slow-roll approximation [Baumann and McAllister \(2015\)](#); [López et al. \(2021\)](#); [Leyva et al. \(2022\)](#).

Using these dimensionless parameters together with the background equations (6) and (8), one gets

$$\epsilon = \delta_X - \frac{1}{2} \delta_U + \frac{1}{2} \delta_{\dot{U}} \delta_U. \quad (10)$$

To first order in slow-roll expansion, this reduces to

$$\epsilon = \delta_X - \frac{1}{2} \delta_U + \mathcal{O}(\epsilon^2), \quad (11)$$

with $\delta_X, \delta_U \ll 1$.

Within the slow-roll approximation, the Friedmann and Klein-Gordon (KG) equations reduce to

$$H^2 \simeq \frac{\kappa V}{3U}, \quad (12)$$

$$\frac{\dot{\phi}}{H} \simeq \frac{2U'}{\kappa} - \frac{V'}{3H^2}. \quad (13)$$

Therefore, to quantify the amount of inflation, we introduce the number of e -folds N defined as

$$N \equiv \int_{\phi_i}^{\phi_f} H dt = \int_{\phi_i}^{\phi_f} \frac{\kappa}{2U' - U \frac{V'}{V}} d\phi. \quad (14)$$

In this latter equation, the field value at the end of inflation is calculated from the condition $\epsilon(\phi_f) = 1$ in (11), and ϕ_i denotes the field value at horizon crossing ($\phi_i \equiv \phi_*$).

2.2. Primordial Fluctuations

2.2.1. Scalar perturbations

In order to study the evolution of primordial perturbations, we work in the unitary gauge, defined by $\delta\phi = 0$. In this gauge, the scalar-perturbed FLRW metric can be written as [De Felice and Tsujikawa \(2011\)](#)

$$ds^2 = -\left[(1 + \alpha)^2 - a(t)^{-2}e^{-2\mathcal{R}}(\partial\psi)^2\right]dt^2 + 2\partial_i\psi dt dx^i + a(t)^2 e^{2\mathcal{R}}\delta_{ij}dx^i dx^j, \quad (15)$$

where α, ψ are nondynamical modes, and \mathcal{R} is the curvature perturbation. Here $(\partial\psi)^2 \equiv \delta^{ij}\partial_i\psi\partial_j\psi$.

Substituting the perturbed metric (15) into the action (1), and expanding to second order, we integrate by parts and eliminate the nondynamical modes, obtaining

$$S = \int dt d^3x a^3 Q_s \left[\mathcal{R}^2 - \frac{c_s^2}{a^2} (\partial\mathcal{R})^2 \right], \quad (16)$$

where

$$Q_s = \frac{w_1(4w_1w_3 + 9w_2^2)}{3w_2^2}, \quad c_s^2 = \frac{3(2w_1^2w_2H - w_2^2w_1 + 4w_1\dot{w}_1w_2 - 2w_1^2\dot{w}_2)}{w_1(4w_1w_3 + 9w_2^2)}, \quad (17)$$

with

$$w_1 = \frac{U}{\kappa}, \quad (18)$$

$$w_2 = \frac{2HU}{\kappa} + \frac{\dot{\phi}}{\kappa}U', \quad (19)$$

$$w_3 = -\frac{9H^2U}{\kappa} + 3X - \frac{9H\dot{\phi}}{\kappa}U'. \quad (20)$$

To ensure the stability of scalar perturbations, we impose $Q_s > 0$ (absence of ghosts) and $c_s^2 > 0$ (absence of gradient instabilities). Expanding Q_s and c_s^2 to leading order in the slow-roll parameters, we obtain

$$Q_s \simeq \frac{U\delta_X}{\kappa}, \quad c_s^2 \simeq 1. \quad (21)$$

After quantizing the curvature perturbation on a quasi-de Sitter background and solving the Mukhanov-Sasaki equation, the scalar power spectrum evaluated at sound-horizon crossing ($c_s k = aH$) is [De Felice et al. \(2011\)](#)

$$\begin{aligned} \mathcal{P}_s &= \frac{H^2}{8\pi^2 Q_s c_s^3} \Big|_{c_s k = aH} = \frac{H^2}{8\pi^2 M_{Pl}^2 U c_s \epsilon_s} \Big|_{c_s k = aH}, \\ &\simeq \frac{\kappa H^2}{8\pi^2 U \delta_X} \Big|_{c_s k = aH}, \end{aligned} \quad (22)$$

where we have also defined

$$\epsilon_s \equiv \frac{\kappa Q_s c_s^2}{U} \simeq \delta_X. \quad (23)$$

The corresponding spectral index reads

$$n_s - 1 \equiv \frac{d \ln \mathcal{P}_s}{d \ln k} \Big|_{c_s k = aH} \simeq -2\epsilon - \delta_U - \eta_s, \quad (24)$$

where

$$\eta_s \equiv \frac{\dot{\epsilon}_s}{H\epsilon_s}. \quad (25)$$

Here η_s quantifies the fractional variation of ϵ_s per Hubble time. The spectral tilt is evaluated at sound-horizon crossing, keeping only first-order slow-roll contributions.

Also, a useful parameter is the running of the scalar spectral index, which is defined as

$$\alpha_s \equiv \frac{dn_s}{d \ln k} \Big|_{c_s k = aH}, \quad (26)$$

whose value is also constrained by the latest observational data.

2.2.2. Tensor perturbations

For tensor perturbations, we consider the transverse-traceless (TT) deformation of the spatial metric [De Felice and Tsujikawa \(2011\)](#),

$$ds^2 = -dt^2 + a^2(t) (\delta_{ij} + h_{ij}) dx^i dx^j, \quad (27)$$

where h_{ij} satisfies

$$\partial^i h_{ij} = 0, \quad h^i_i = 0. \quad (28)$$

Tensor perturbations can be decomposed into the two polarization states as [Baumann and McAllister \(2015\)](#)

$$h_{ij} = h_+ e_{ij}^+ + h_\times e_{ij}^\times, \quad (29)$$

which leads to the quadratic action

$$S_t^{(2)} = \sum_{p=\pm, \times} \int dt d^3x a^3 Q_t \left[\dot{h}_p^2 - \frac{c_t^2}{a^2} (\partial h_p)^2 \right], \quad (30)$$

with

$$Q_t = \frac{w_1}{4}, \quad c_t^2 = 1. \quad (31)$$

Hence, tensor modes propagate at the speed of light and are free of gradient instabilities, while the no-ghost condition requires $Q_t > 0$. The tensor power spectrum, evaluated at horizon crossing, is [De Felice and Tsujikawa \(2011\)](#)

$$\mathcal{P}_t = \frac{H^2}{2\pi^2 Q_t c_t^3} \Big|_{c_s k = aH}. \quad (32)$$

The corresponding tensor tilt is

$$n_t \equiv \frac{d \ln \mathcal{P}_t}{d \ln k} \Big|_{c_s k = aH} = -2\epsilon - \delta_U. \quad (33)$$

Finally, the tensor-to-scalar ratio reads

$$r = \frac{\mathcal{P}_t}{\mathcal{P}_s} = 16c_s \epsilon_s \simeq -8n_t, \quad (34)$$

showing that r and n_t are not independent.

3. Effective dynamics in LQC with non-minimal coupling

3.1. Effective equations and bounce

In loop quantum cosmology, it is convenient to work with the canonical pair adapted to isotropic geometries [Agullo and Corichi \(2014\)](#); [Bojowald \(2005, 2004\)](#); [Gambini and Pullin \(2011\)](#); [Thiemann \(2007\)](#)

$$|p| := a^2, \quad c := \gamma \dot{a}, \quad (35)$$

where γ is the Barbero-Immirzi parameter. For later convenience, we also introduce

$$\pi := a^3 \dot{\phi} = p^{3/2} \dot{\phi}, \quad (36)$$

which should not be confused with the canonical momentum of ϕ , $\pi_\phi = \partial \mathcal{L} / \partial \dot{\phi} = \pi - (3/\kappa) a^3 H U'$, in the presence of the non-minimal coupling.

In terms of (p, c, ϕ, π) , the mini-superspace Lagrangian can be written as

$$\mathcal{L} = -\frac{3}{\kappa \gamma^2} \sqrt{p} c^2 U - \frac{3}{\kappa \gamma} p c U' \dot{\phi} + \frac{\pi^2}{2p^{3/2}} - p^{3/2} V, \quad (37)$$

leading to the Hamiltonian

$$\mathcal{H} = -\frac{3}{\kappa\gamma^2} \sqrt{p} c^2 U - \frac{3}{\kappa\gamma} p c U' \dot{\phi} + \frac{\pi^2}{2p^{3/2}} + p^{3/2} V. \quad (38)$$

Quantum-geometry effects are incorporated at the effective level by (i) implementing holonomy corrections, $c \rightarrow \sin(\mu_0 c)/\mu_0$ Artymowski et al. (2013); Bojowald and Kagan (2006), where μ_0 represents the ‘‘length’’ of the edge along which the holonomy is computed, and (ii) including inverse-volume corrections encoded in the function $D_l(q)$ Germani et al. (2007); Bojowald (2001); Bojowald et al. (2004); Bojowald (2002b). The resulting effective Hamiltonian reads

$$\mathcal{H}_{LQ} = -\frac{3}{\kappa\gamma^2 \mu_0^2} \sqrt{p_{LQ}} \sin^2(\mu_0 c_{LQ}) U - \frac{3}{\kappa\gamma^2 \mu_0} p_{LQ} \sin(\mu_0 c_{LQ}) U' \dot{\phi}_{LQ} + D_l^{-(n+1)} \frac{\pi_{LQ}^2}{2p_{LQ}^{3/2}} + D_l^m p_{LQ}^{3/2} V. \quad (39)$$

The inverse-volume factor arises from the expectation values of the volume and inverse-volume operators,

$$\langle \widehat{a^3} \rangle = a_{LQ}^3, \quad \langle \widehat{a^{-3}} \rangle = D_l(q) a_{LQ}^{-3}, \quad (40)$$

with $q \equiv a_{LQ}^2/a_{Pl}^2$ and a_{Pl} denoting the scale factor at the quantum-to-classical transition. The explicit form of $D_l(q)$ is Germani et al. (2007)

$$D_l(q) = \left\{ \frac{3q^{l-1}}{2l} \left[\frac{(q+1)^{l+2} - |q-1|^{l+2}}{l+2} - \frac{q}{1+l} \left((q+1)^{l+1} - \text{sgn}(q-1)|q-1|^{l+1} \right) \right] \right\}^{\frac{3}{2-2l}}. \quad (41)$$

Upon quantization, operator-ordering ambiguities allow one to split powers of a in different ways. Parametrizing this freedom by (m, n) , one finds schematically Germani et al. (2007)

$$\begin{aligned} a_{LQ}^3 &= a_{LQ}^{3(m+1)} a_{LQ}^{-3m} \rightarrow \langle \widehat{a^3} \rangle^{(m+1)} \langle \widehat{a^{-3}} \rangle^m = D_l^m a_{LQ}^3, \\ a_{LQ}^{-3} &= a_{LQ}^{-3(n+1)} a_{LQ}^{3n} \rightarrow \langle \widehat{a^{-3}} \rangle^{(n+1)} \langle \widehat{a^3} \rangle^n = D_l^{-(n+1)} a_{LQ}^3. \end{aligned} \quad (42)$$

The parameters m and n are not fixed by a unique ordering prescription, but their physical impact is entirely governed by the profile of the correction factor $D_l(q)$. In the deep quantum regime near the bounce, $D_l(q)$ deviates strongly from its classical limit. This behavior is illustrated in the left panel of FIG. 1 for the standard parameter choice $l = 3/4$ over the narrow domain $q \in [0, 3]$, clearly highlighting the quantum-to-classical transition that occurs around $q = 1$. Conversely, in the classical macroscopic regime ($q \gg 1$), the discrete quantum geometry is coarse-grained, and one recovers $D_l \rightarrow 1$, naturally switching off the corrections. The right panel demonstrates this asymptotic behavior over a broader range up to $q = 150$. Crucially, in our cosmological setup, the horizon crossing of observable scales occurs around $q = 100$. This confirms that the primordial perturbations are generated deep within the quasi-classical regime, where the inverse-volume effects provide small, perturbative modifications rather than dominating the background dynamics.

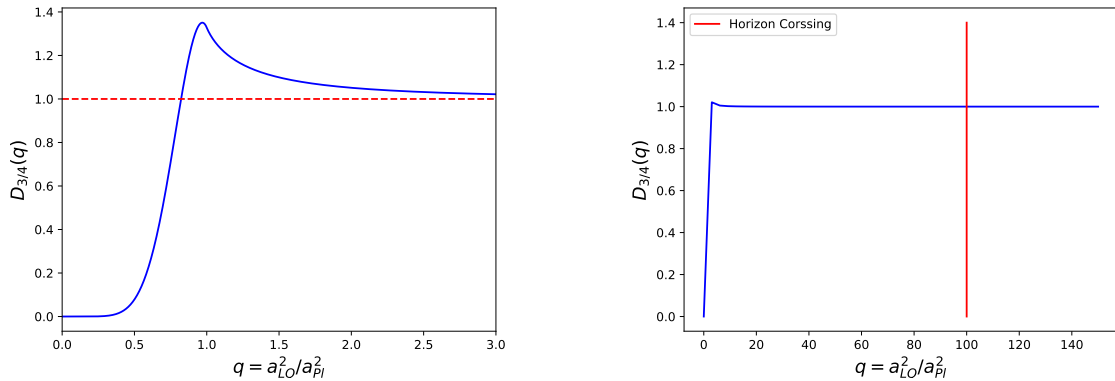


Figure 1: Inverse-volume correction $D_l(q)$ as a function of q , shown for $l = 3/4$.

At the quantum level, physical states satisfy the Hamiltonian constraint

$$\widehat{\mathcal{H}}_{LQ} |\Phi\rangle = 0, \quad (43)$$

with

$$\begin{aligned} \widehat{\mathcal{H}}_{LQ} = & -\frac{3}{\kappa\gamma^2\mu_0^2} \left(\widehat{p^{3/2}}\right)^{1/3} \left(\widehat{\sin(\mu_0 c)}\right)^2 \widehat{U} - \frac{3}{\kappa\gamma^2\mu_0} \left(\widehat{p^{3/2}}\right)^{1/3} \widehat{\sin(\mu_0 c)} \widehat{U}' \widehat{\pi} \\ & + \left(\widehat{p^{-3/2}}\right)^{(n+1)} \left(\widehat{p^{3/2}}\right)^n \frac{\widehat{\pi}^2}{2} + \left(\widehat{p^{3/2}}\right)^{(m+1)} \left(\widehat{p^{-3/2}}\right)^m \widehat{V}. \end{aligned} \quad (44)$$

Here, the parameters m and n encode the usual quantization ambiguity associated with how powers of the scale factor are distributed among operators in the prefactors of the kinetic and potential terms. In addition, the gravitational sector entails an operator-ordering ambiguity because the triad and holonomy operators do not commute. In particular,

$$[\widehat{p}, e^{i\mu_0 c}] = \frac{8\pi\gamma\ell_p^2\mu_0}{3} e^{i\mu_0 c}, \quad [\widehat{\phi}, \widehat{\pi}_\phi] = i, \quad (45)$$

so different orderings of \widehat{p} and holonomy operators (or \widehat{p} and $\widehat{\pi}$) lead to inequivalent realizations of the quantum constraint. Although this second source of ambiguity is typically negligible at the characteristic energy scales of slow-roll inflation, it plays a crucial role in the deep quantum regime, where the detailed operator ordering influences the construction of the physical state space and the definition of the physical vacuum state.

In the classical limit, one recovers the standard Hamiltonian constraint $\langle \widehat{\mathcal{H}} \rangle = 0$ by taking $D_l \rightarrow 1$ and $\sin(\mu_0 c) \rightarrow \mu_0 c$, together with the replacement of operators by their classical counterparts (and commutators by Poisson brackets).

3.2. Slow-roll regime and number of e -folds

We restrict ourselves to the quasi-classical regime $\mu_0|c| \ll 1$, so that $\sin(\mu_0 c) \simeq \mu_0 c$ and holonomy corrections can be neglected. In this limit, the only LQC corrections we retain are the inverse-volume effects encoded in $D_l(q)$, which may still be relevant near the quantum-to-classical transition.

In this limit, the effective Hamiltonian constraint reduces to

$$-\frac{3}{\kappa} H_{LQ} [H_{LQ} U + \dot{\phi}_{LQ} U'] + D_l^{-(n+1)} \frac{\dot{\phi}_{LQ}^2}{2} + D_l^m V = 0, \quad (46)$$

which plays the role of the LQC-modified Friedmann equation.

It is also convenient to work with the corresponding effective Lagrangian,

$$\mathcal{L}_{LQ} = a_{LQ}^3 \left[-\frac{3}{\kappa} H_{LQ} (H_{LQ} U + \dot{\phi}_{LQ} U') + D_l^{-(n+1)} \frac{\dot{\phi}_{LQ}^2}{2} - D_l^m V \right], \quad (47)$$

from which we obtain the LQG-corrected Klein-Gordon equation

$$-\frac{3U'}{\kappa} \left[\left(\frac{\ddot{a}}{a} \right)_{LQ} + H_{LQ}^2 \right] + D_l^{-(n+1)} \left[\ddot{\phi}_{LQ} + 3H_{LQ} \dot{\phi}_{LQ} - (n+1) \left(\frac{\dot{D}_l}{D_l} \right) \dot{\phi}_{LQ} \right] + D_l^m V' = 0, \quad (48)$$

together with the second (Raychaudhuri-type) Friedmann equation

$$\frac{1}{\kappa} \left[2U \left(\frac{\ddot{a}}{a} \right)_{LQ} + H_{LQ} (2U' \dot{\phi}_{LQ} + H_{LQ} U) + \dot{\phi}_{LQ}^2 U'' + \ddot{\phi}_{LQ} U' \right] + D_l^{-(n+1)} \frac{\dot{\phi}_{LQ}^2}{2} - D_l^m V = 0. \quad (49)$$

Implementing the LQC-modified slow-roll conditions in (9) and defining

$$\begin{aligned} (\delta_D)_{LQ} & \equiv \frac{\dot{D}_l}{H_{LQ} D_l} = \delta_D \\ & = \frac{3 \left[(q+1)^l (l^2 - 3lq + 3q^2 - 1) - (q-1)^l (l^2 + 3lq + 3q^2 - 1) \right]}{(l-1) [(l+q+1)(q-1)^{l+1} + (l-q+1)(q+1)^{l+1}]}, \end{aligned} \quad (50)$$

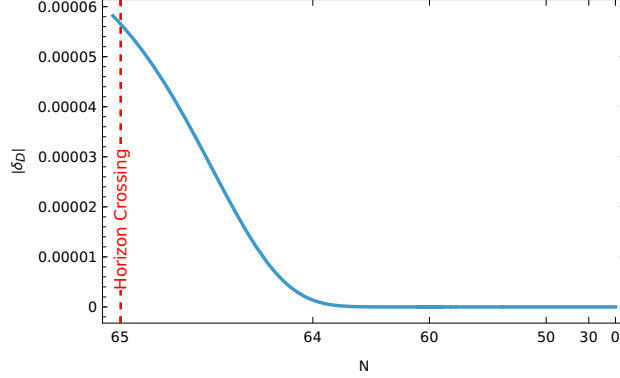


Figure 2: Evolution of δ_D with number of e-fold N for $l = 3/4$

we get the 0th order Friedmann equation¹

$$H_{LQ}^2 = \kappa D_l^m \frac{V}{3U} = D_l^m H^2, \quad (51)$$

and the 0th order Klein-Gordon equation

$$\frac{\dot{\phi}_{LQ}}{H_{LQ}} = \frac{1}{3} D_l^{-(n+1)} \left[\frac{6U'}{\kappa} - \frac{D_l^m V'}{H_{LQ}^2} \right] = D_l^{-(n+1)} \frac{\dot{\phi}}{H}. \quad (52)$$

As illustrated in FIG. 2, the parameter δ_D captures the fractional rate of change of the inverse-volume correction over a Hubble time. In the immediate post-bounce phase, during the quantum-to-classical transition near $q \sim 1$, $D_l(q)$ varies rapidly, making δ_D a dynamically significant quantity. However, as the universe expands and successfully enters the inflationary regime ($q \gg 1$), the effective geometry smooths out, and D_l approaches unity. Consequently, its time derivative naturally diminishes, and δ_D asymptotically vanishes ($\delta_D \rightarrow 0$). Because both δ_D and its time variation over a Hubble time remain sufficiently small throughout the observable e -folding window, δ_D behaves mathematically just like a standard kinematic slow-roll parameter, allowing it to be consistently incorporated into the first-order perturbative expansion.

These expressions, Eq. (51) and Eq. (52) allow us to relate the inflaton evolution to the e -folding number N_{LQ} via

$$\begin{aligned} \frac{d\phi_{LQ}}{dN_{LQ}} &= \frac{1}{3} D_l^{-(n+1)} \left[\frac{6U'}{\kappa} - \frac{D_l^m V'}{H_{LQ}^2} \right], \\ N_{LQ} &= \int_{(\phi_i)_{LQ}}^{(\phi_f)_{LQ}} \frac{3D_l^{(n+1)}}{\left[\frac{6U'}{\kappa} - \frac{D_l^m V'}{H_{LQ}^2} \right]} d\phi_{LQ}. \end{aligned} \quad (53)$$

This relation will be used in the next section to evaluate the inflationary observables at horizon crossing, by expressing all background quantities in terms of the field value (or equivalently N_{LQ}).

3.3. Perturbations and observables

Starting from the second order action (16) and retaining only inverse-volume corrections, we obtain

$$\begin{aligned} (Q_s)_{LQ} &\simeq \left(\frac{U\delta_X}{\kappa} \right)_{LQ} = D_l^{-2(n+1)} \frac{U\delta_X}{\kappa} = D_l^{-2(n+1)} Q_s, \\ (c_s)_{LQ}^2 &\simeq D_l^{-(n+1)} \left(1 - \frac{n+1}{2} \delta_D \right). \end{aligned} \quad (54)$$

¹Note that the unscripted quantities on the right-hand side correspond to their classical functional forms, but are evaluated along the effective LQC trajectory ϕ_{LQ} i.e. $H_{LQ}^2(\phi_{LQ}) = D_l^m H^2(\phi_{LQ})$.

These modifications to the perturbation amplitude can be rigorously understood through the ‘‘dressed metric’’ approach to LQC [Agullo and Corichi \(2014\)](#). In this framework, rather than deforming the constraint algebra of the perturbations, the linear scalar and tensor modes are treated as quantum test fields propagating on a coarse-grained, quantum-corrected effective background. Because the quantum fluctuations of the geometry are traced over to produce a dressed effective metric that preserves the standard Lorentzian causal structure, the perturbations strictly propagate at the speed of light, yielding $(c_s)_{LQ}^2 = 1$. Furthermore, even within the alternative anomaly-free framework where inverse-volume effects explicitly deform the constraint algebra [Bojowald \(2007\)](#); [Parvizi et al. \(2026\)](#), the modified speed of sound is given by Eq. (54). Since the inflationary observables are evaluated at horizon exit deep in the slow-roll regime ($q \gg 1$), the inverse-volume contributions that enter the propagation sector approach their classical limit ($D_l \rightarrow 1$ and $\delta_D \rightarrow 0$), so any deviation of $(c_s)_{LQ}^2$ from unity is higher order. Therefore, at first order, it is consistent in both implementations to adopt an effective $(c_s)_{LQ}^2 \simeq 1$ when computing the primordial power spectra.

Accordingly, the slow-roll parameters entering the spectra rescale as

$$(\delta_U)_{LQ} = D_l^{-(n+1)} \delta_U, \quad (55)$$

$$(\delta_X)_{LQ} = D_l^{m-2(n+1)} \delta_X. \quad (56)$$

and the quantity η_s becomes

$$(\eta_s)_{LQ} = D_l^{-m/2} \eta_s - 2(n+1)\delta_D. \quad (57)$$

The first slow-roll parameter is, therefore,

$$\epsilon_{LQ} \simeq (\delta_X)_{LQ} - \frac{1}{2} (\delta_U)_{LQ} = D_l^{m-2(n+1)} \delta_X - \frac{1}{2} D_l^{-(n+1)} \delta_U. \quad (58)$$

As a result, the scalar power spectrum at horizon crossing $(\phi_{LQ}, q) = ((\phi_i)_{LQ}, q_i)$ becomes

$$(\mathcal{P}_s)_{LQ} = D_l^{m+2(n+1)} \mathcal{P}_s \Big|_{(\phi_i)_{LQ}, q_i}. \quad (59)$$

Therefore, the scalar spectral index reads

$$\begin{aligned} (n_s)_{LQ} - 1 &= -2\epsilon_{LQ} - (\delta_U)_{LQ} - (\eta_s)_{LQ} \Big|_{(\phi_i)_{LQ}, q_i}, \\ &= -2D_l^{-(n+1)} \delta_X - D_l^{-m/2} \eta_s + 2(n+1)\delta_D \Big|_{(\phi_i)_{LQ}, q_i}. \end{aligned} \quad (60)$$

Finally, the tensor-to-scalar ratio is corrected according to

$$r_{LQ} = D_l^{-2(n+1)} r \Big|_{(\phi_i)_{LQ}, q_i}. \quad (61)$$

Having established the effective post-bounce dynamics, we now assess the typicality of a sufficiently long slow-roll phase by using the Liouville measure on the space of solutions to compute the fraction of trajectories with $N \geq N_\star$.

3.4. Probability of inflation from the induced Liouville measure

The probability of inflation is defined using the Liouville measure and its induced measure on the constraint surface after gauge fixing [Schiffin and Wald \(2012\)](#); [Gibbons and Turok \(2008\)](#). Details are given in Appendix [Appendix A](#). We parametrize the effective constraint surface by $Q^i = \{\phi, q \equiv a^2/a_{\text{Pl}}^2, H\}$.

For the effective Lagrangian in Eq. (47), the conjugate momenta are defined as

$$P_{Q^i} = \frac{\partial \langle \mathcal{L}_{LQ} \rangle}{\partial \dot{Q}^i}. \quad (62)$$

In particular, one finds

$$\begin{aligned} P_{\phi_{LQ}} &= a_{\text{Pl}}^3 q^{3/2} \left(D_l^{-(n+1)} \dot{\phi}_{LQ} - \frac{3}{\kappa} H_{LQ} U' \right), \\ P_{H_{LQ}} &= 0. \end{aligned} \quad (63)$$

Following Refs. Nelson (2007); Germani et al. (2007); Ashtekar and Sloan (2011b), we introduce the vector potential

$$\mathbf{A} = (P_{\phi_{LQ}}, P_{H_{LQ}}, P_q), \quad (64)$$

and the associated divergence-free field

$$\mathbf{B} = \nabla \times \mathbf{A}. \quad (65)$$

This formulation is equivalent to pulling back the Liouville measure to the Hamiltonian constraint surface and evaluating the induced measure on a transversal section. Restricting to the constant- q hypersurface $q = q_s$, the corresponding measure element can be written as the flux element $B_q dH_{LQ} d\phi_{LQ}$ Schiffrin and Wald (2012); Gibbons and Turok (2008).

The normalization factor is then defined as

$$\mathcal{N} = \int \int B_q dH_{LQ} d\phi_{LQ}, \quad (66)$$

where B_q denotes the q -component of \mathbf{B} . The probability of inflation is given by the ratio Gibbons and Turok (2008); Gibbons et al. (1987)

$$\mathcal{P} = \frac{\mathcal{M}}{\mathcal{N}}, \quad (67)$$

with

$$\mathcal{M} = \int \int B_q dH_{LQ} d\phi_{LQ} \Big|_{\text{inflation}}. \quad (68)$$

For our effective dynamics, one obtains

$$B_q = a_{\text{Pl}}^3 q^{3/2} \left[\frac{D_l^m V'}{3H_{LQ}^2} - \frac{U'}{\kappa} \right]. \quad (69)$$

Equivalently, the probability of obtaining an inflationary phase within a specified range of initial data can be written as Bedić and Vereshchagin (2019)

$$\mathcal{P}(N_{LQ}, \phi_{LQ}) = \frac{1}{Z} \left| \int_{(\phi_i)_{LQ}}^{(\phi_f)_{LQ}} \int_{(H_i)_{LQ}}^{(H_f)_{LQ}} B_q dH_{LQ} d\phi_{LQ} \right|, \quad (70)$$

where Z is a normalization constant (of the same nature as \mathcal{N}).

In the following section we specialize this probabilistic framework to Higgs inflation with a non-minimal coupling. We derive the corresponding effective background dynamics and inflationary observables, and then use the induced Liouville measure introduced above to quantify the fraction of trajectories that produce a sufficiently long inflationary phase.

Only the inverse-volume corrected quantities will be evaluated for the analysis. Henceforth we will drop the subscript “ LQ ” for convenience.

4. Higgs inflation with non-minimal coupling

We consider the standard non-minimal coupling function

$$U(\phi) = 1 + \xi\phi^2, \quad (71)$$

together with a Higgs-like quartic potential

$$V(\phi) = \lambda(\phi^2 - v_0^2)^2. \quad (72)$$

Identifying the inflaton field with the Higgs field as the inflaton is motivated by minimality, since it utilizes the only fundamental scalar field already observed in nature, requiring no new particle degrees of freedom beyond the Standard Model. In the absence of a non-minimal coupling ($\xi = 0$), the quartic potential $V(\phi) \propto \phi^4$ is disfavored by current CMB constraints, as it generically predicts a tensor-to-scalar ratio r that is too large. However, introducing a non-minimal coupling term $\xi\phi^2 R$ effectively flattens the potential in the Einstein frame, leading to values of (n_s, r) compatible with observations. Furthermore, recent ACT DR6 results [Louis et al. \(2025\)](#); [Calabrese et al. \(2025\)](#); [Ellis et al. \(2025\)](#), particularly when combined with Planck and DESI [Kallosh et al. \(2025\)](#); [Maity \(2025\)](#); [Kumar et al. \(2025\)](#), mildly favor a slightly larger scalar spectral index (with a representative value $n_s \simeq 0.974$). This upward shift can introduce tension for standard plateau-type models, while Higgs inflation may remain compatible once quantum-gravity corrections are taken into account.

Therefore, in the remainder of this work, we quantify how LQC effective corrections modify the dynamics and the predicted observables of non-minimally coupled Higgs inflation, and we assess whether the resulting (n_s, r) remain compatible with current CMB constraints. These results will then be used to evaluate, within the Liouville-measure framework introduced above, the probability of obtaining a sufficiently long inflationary phase.

During inflation one typically has $|\phi| \gg v_0$, so the symmetry-breaking scale is negligible. Accordingly, in the following, we set $v_0 \simeq 0$.

4.1. Cosmological perturbation

For the non-minimal coupling (71) and the Higgs potential (72), the slow-roll quantities defined in (9) take the form

$$\delta_U = -\frac{8\xi D_l^{-(n+1)}}{\kappa(1 + \xi\phi^2)}, \quad (73)$$

$$\delta_X = \frac{8D_l^{m-2(n+1)}}{\kappa\phi^2(1 + \xi\phi^2)}. \quad (74)$$

Substituting these expressions into (11), we obtain the first slow-roll parameter

$$\epsilon \simeq \frac{4D_l^{-2(n+1)}(2D_l^m + \xi\phi^2 D_l^{n+1})}{\kappa\phi^2(1 + \xi\phi^2)}. \quad (75)$$

The inflaton value at the end of inflation, ϕ_f , is determined by the condition $\epsilon = 1$, which yields

$$\phi_f^2 = \frac{\sqrt{\kappa^2 + 24\kappa\xi + 16\xi^2} - (\kappa - 4\xi)}{2\kappa\xi}. \quad (76)$$

At the level of the algebraic equation for ϕ_f^2 , there are two roots. We select the physically admissible one with $\phi_f^2 > 0$.

We define another slow-roll parameter analogous to Eq. (23)

$$\epsilon_s \equiv \frac{\kappa Q_s c_s^2}{U} \simeq (\delta_X)_{LQ}, \quad (77)$$

Evaluated at horizon crossing $(\phi, q) = (\phi_i, q_i)$, the scalar power spectrum is

$$\mathcal{P}_s = D_l^{m+2(n+1)} \frac{\kappa^3 \lambda \phi^6}{192\pi^2 (\xi\phi^2 + 1)} \Big|_{\phi=\phi_i, q=q_i}. \quad (78)$$

From this latter expression, we can solve the self-coupling parameter $\lambda(N_*)$ as a function of the scalar field value at the horizon crossing $\phi_* = \phi(N_*)$. Using the latest observational constraints, we consider the value $P_s = 2.141 \times 10^{-9}$ Akrami et al. (2020).

So, the scalar spectral index and tensor-to-scalar ratio are

$$n_s - 1 = \frac{D_l^{-\frac{m}{2}} \left[2\phi^2 \left(\kappa(n+1)\delta_D(\xi\phi^2 + 1) - 8\xi \right) - 8 \right] - 16D_l^{-(n+1)}}{\kappa\phi^2(1 + \xi\phi^2)} \Bigg|_{\phi=\phi_i, q=q_i}, \quad (79)$$

$$r = \frac{128D_l^{m-2(n+1)}}{\kappa\phi^2(1 + \xi\phi^2)} \Bigg|_{\phi=\phi_i, q=q_i}.$$

Finally, using eq. (26), the running of the spectral index is computed as

$$\alpha_s = \frac{dn_s}{dN} = \frac{64\xi^2}{A_4^2(A_4 + \kappa)^2} \left[D_l^{(n+1)-\frac{m}{2}} (2\kappa A_4 + 2A_4^2 + \kappa^2) + 2\kappa(2A_4 + \kappa) \right] \Bigg|_{q=q_i, N=N_i}, \quad (80)$$

where A_4 is defined as

$$A_4 \equiv D_l^{n+1} \xi (\kappa\phi_f^2 + 8N). \quad (81)$$

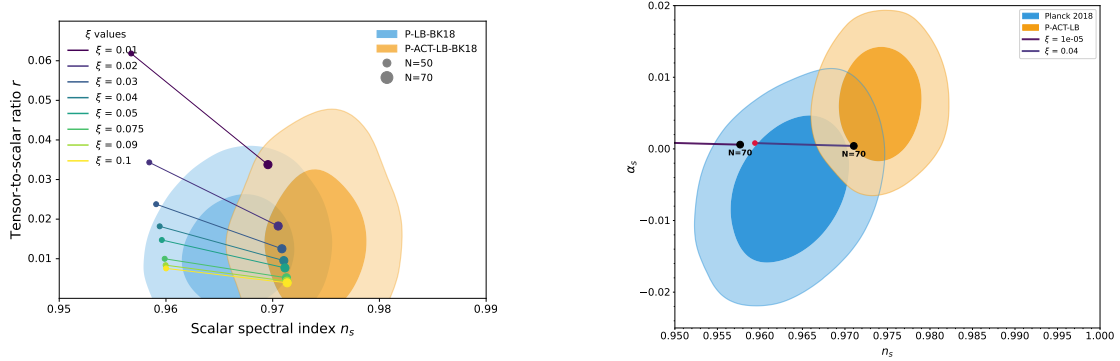


Figure 3: Inflationary predictions for $V(\phi) \propto \phi^4$ in LQC with inverse-volume corrections. Left panel shows r versus n_s and right panel shows α_s versus n_s for different non-minimal couplings ξ , with markers at $N = 50$ and $N = 70$. We fix the operator-ordering parameters $m = 0$, $n = 0$, the inverse-volume eigenvalue parameter $l = 3/4$, and the initial value $q_i = 100$.

FIG. 3 summarizes our predictions for the quartic potential $V(\phi) \propto \phi^4$ in LQC, including inverse-volume corrections. The left panel shows the (n_s, r) plane for several values of the non-minimal coupling ξ , while the right panel shows the corresponding trajectories in the (n_s, α_s) plane. The dots indicate the predictions evaluated at $N = 50$ and $N = 70$ e-folds. Throughout, we fix the operator-ordering parameters to $m = 0$ and $n = 0$, choose $l = 3/4$, and set the initial value $q_i = 100$. Our predictions are compared with the Planck 2018 and ACT+Planck+BICEP/Keck constraints, shown as shaded contours. FIG. 4 complements this comparison by translating the observational bounds into constraints on the model parameters. Specifically, we project the viable solutions onto the (N, ξ) plane and retain only those points that simultaneously satisfy the bounds in the (n_s, r) and (n_s, α_s) planes. We also impose the lower limit $r \gtrsim 5 \times 10^{-4}$ Franciolini et al. (2019). This representation makes explicit the allowed ranges of ξ and the corresponding number of e-folds consistent with current data.

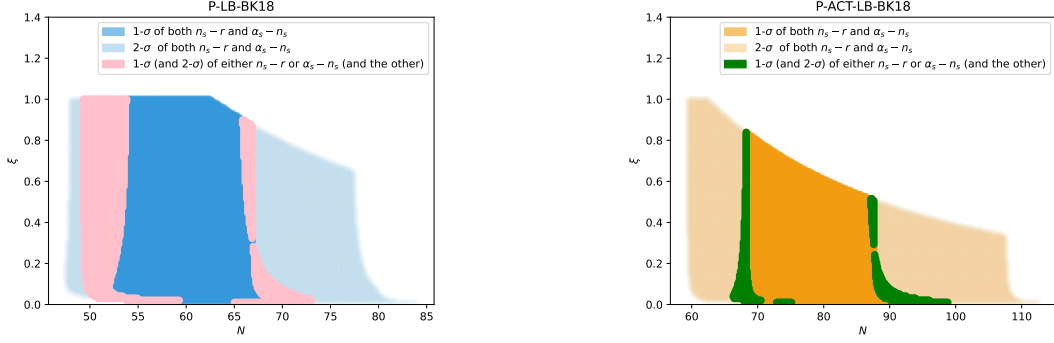


Figure 4: Allowed region in the (N, ξ) plane for the quartic potential $V(\phi) \propto \phi^4$ in LQC with inverse-volume corrections, imposing the theoretical bound $r \gtrsim 5 \times 10^{-4}$ [Franciolini et al. \(2019\)](#). The left panel uses P-LB-BK18 constraints and the right panel uses P-ACT-LB-BK18 constraints. We fix the operator-ordering parameters $m = 0$ and $n = 0$, the inverse-volume eigenvalue parameter $l = 3/4$, and the initial value $q_i = 100$.

We now use these LQC-corrected observables to evaluate, within the Liouville-measure framework, the fraction of initial conditions that yield sufficient inflation.

4.2. Probability of inflation

In the slow-roll regime, the loop-corrected Hubble parameter takes the form

$$H^2 = D_l^m \frac{\kappa \lambda (\phi^2 - v_0^2)^2}{3(1 + \xi \phi^2)}. \quad (82)$$

The evolution of the inflaton in terms of the number of e-folds follows from Eq. (53). For the present choice of potential and non-minimal coupling, we find

$$\frac{d\phi}{dN} = -4D_l^{(n+1)} \frac{\phi(1 + \xi v_0^2)}{\kappa(\phi^2 - v_0^2)}, \quad (83)$$

and thus²

$$N = \frac{\kappa}{8(1 + \xi v_0^2)} \left[2v_0^2 \log \left(\frac{\phi_f}{(\phi_i)^{D_l(q_i)^{-(n+1)}}} \right) + (D_l(q_i)^{-(n+1)} \phi_i^2 - \phi_f^2) \right]. \quad (84)$$

The momentum conjugate to ϕ is given by

$$P_\phi = a_{\text{Pl}}^3 q^{3/2} \left(\dot{\phi} D_l^{-(n+1)} - \frac{6H\xi\phi}{\kappa} \right), \quad (85)$$

and it is convenient to introduce the auxiliary quantity

$$B_q = a_{\text{Pl}}^3 q^{3/2} \frac{(4D_l^m \kappa \lambda \phi (\phi^2 - v_0^2) - 6H^2 \xi \phi)}{3H^2 \kappa}. \quad (86)$$

The probability of realizing a sufficiently long inflationary phase is proportional to the corresponding Liouville measure \mathcal{M} on the space of solutions. By using (70), we thus obtain

$$\mathcal{P} \propto 2a_{\text{Pl}}^3 q^{3/2} \sqrt{\frac{\lambda}{3\kappa}} \left[\sqrt{(\xi \phi_i^2 + 1)(\phi_i^2 - v_0^2)^2 D_l(q_i)^m} - \sqrt{(\xi \phi_f^2 + 1)(\phi_f^2 - v_0^2)^2} \right], \quad (87)$$

²Here, we use integration by parts to pull D_l out of the integral: $\int D_l f(\phi) d\phi = D_l \int f(\phi) d\phi - \int \delta_D D_l \frac{H}{\phi} \left(\int f(\phi) d\phi \right) d\phi$. Since δ_D is a small first-order parameter in the slow-roll expansion, the second term is strictly higher-order. Therefore, to zeroth order, we can safely approximate $\int D_l f(\phi) d\phi \approx D_l \int f(\phi) d\phi$.

where $D_l(q_f) \rightarrow 1$ is the classical limit.

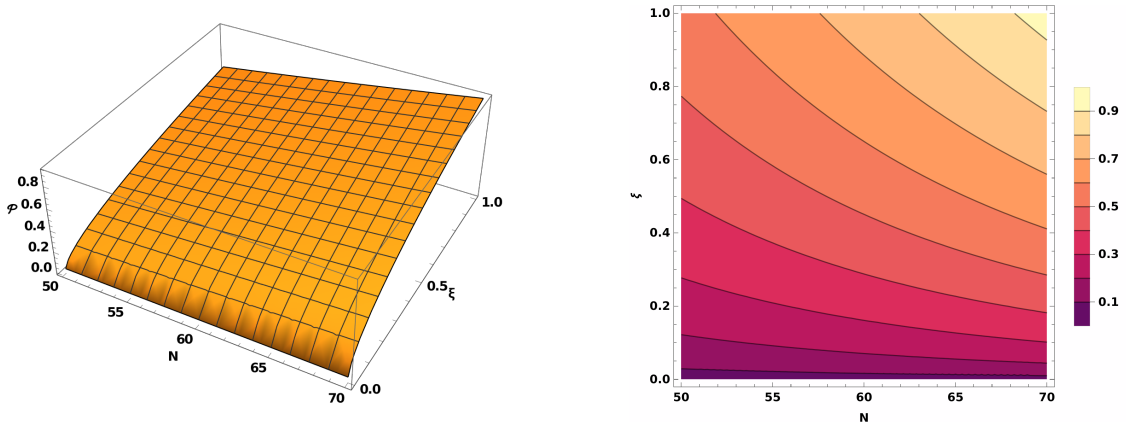


Figure 5: Effect of the non-minimal coupling parameter ξ on the probability of inflation \mathcal{P} for the quartic potential $V(\phi) = \lambda\phi^4$, with $\lambda \simeq 6.14 \times 10^{-13}$ inferred from the scalar power-spectrum amplitude $\mathcal{P}_s = 2.141 \times 10^{-9}$ Akrami et al. (2020). The left panel shows the surface $\mathcal{P}(N, \xi)$ and the right panel shows the corresponding contour map. We fix the inverse-volume eigenvalue parameter to $l = 3/4$ and the initial value to $q_i = 100$.

To quantify the typicality of a successful slow-roll phase, we evaluate the Liouville measure of the effective phase space for the quartic potential. FIG. 5 shows how the probability of achieving a given number of e-folds, N , depends on the non-minimal coupling ξ , with the self-coupling λ held fixed to correctly normalize the amplitude of the scalar power spectrum, $\mathcal{P}_s = 2.141 \times 10^{-9}$ Akrami et al. (2020). Notably, for this Higgs-like potential, the probability of sufficient inflation exhibits a strong enhancement as the non-minimal coupling ξ increases. The left panel provides a three-dimensional representation of the probability distribution, while the right panel shows the corresponding contour map. It is worth emphasizing that while these plots explore a broad theoretical parameter domain—specifically $\xi \in (0, 1)$ and $N \in (0, 70)$ in units where $M_{pl}^2 = 1$ —only a strictly bounded, highly localized subset of this space actually aligns with physical trajectories that satisfy current CMB bounds.

5. String-inspired potentials with non-minimal coupling

In this section, we investigate string-motivated fractional monomial potentials in the presence of a non-minimal coupling to gravity. We adopt the coupling function given in Eq. (71) and focus on the two representative potentials

$$V(\phi) = \begin{cases} \lambda\phi^{1/3} \\ \lambda\phi^{2/3} \end{cases} . \quad (88)$$

Monomial potentials of the form $V(\phi) \propto \phi^p$ with fractional powers $p < 1$ are strongly motivated by ultraviolet (UV) completions of inflation, particularly within the framework of string theory. For instance, axion monodromy inflation naturally generates such potentials, where the underlying shift symmetry of an axion field is broken by branes or fluxes, leading to a flattened potential structure. These “flattened” potentials are phenomenologically advantageous because they predict a significantly lower tensor-to-scalar ratio r compared to standard chaotic inflation ($p = 2, 4$), placing them comfortably within the precision bounds set by Planck and BICEP/Keck. Additionally, the recent trend in ACT DR6 observational data towards slightly larger n_s values renews interest in these fractional power laws, as they occupy a favorable region of the $n_s - r$ plane that is distinct from the Starobinsky or Higgs attractors.

5.1. Cosmological perturbation

5.1.1. $V(\phi) = \lambda\phi^{1/3}$

For the fractional monomial potential $V(\phi) = \lambda\phi^{1/3}$, the loop-corrected slow-roll parameters take the form

$$\begin{aligned}\delta_X &= \frac{(1 - 11\xi\phi^2)^2 D_l^{m-2(n+1)}}{18\phi^2 (\kappa\xi\phi^2 + \kappa)}, \\ \delta_U &= \frac{2\xi(11\xi\phi^2 - 1) D_l^{-(n+1)}}{3(\kappa\xi\phi^2 + \kappa)}, \\ \epsilon &= -\frac{(11\xi\phi^2 - 1) D_l^{-2(n+1)} \left((1 - 11\xi\phi^2) D_l^m + 6\xi\phi^2 D_l^{n+1} \right)}{18\phi^2 (\kappa\xi\phi^2 + \kappa)}.\end{aligned}\quad (89)$$

Inflation ends when the slow-roll condition is violated, i.e. when $\epsilon \simeq 1$, which yields

$$\phi_f^2 = \frac{1}{3\sqrt{9\kappa^2 + 18\kappa\xi + \xi^2} + 9\kappa + 8\xi}.\quad (90)$$

The corresponding inflationary observables, evaluated at horizon exit ($\phi = \phi_i$, $q = q_i$), are

$$\mathcal{P}_s = D_l^{m+2(n+1)} \frac{3\kappa^3 \lambda \phi^{7/3}}{4\pi^2 (1 - 11\xi\phi^2)^2 (\xi\phi^2 + 1)} \Big|_{\phi=\phi_i, q=q_i},\quad (91)$$

from which we obtain $\lambda(N_*)$ at the horizon crossing, and

$$\begin{aligned}n_s - 1 &= -\frac{2(1 + 13\xi\phi^2) D_l^{-\frac{m}{2}}}{3\kappa\phi^2 (1 + \xi\phi^2)} + 2(n+1)\delta_D D_l^{-\frac{m}{2}} - \frac{(1 - 11\xi\phi^2)^2 D_l^{-(n+1)}}{9\kappa\phi^2 (1 + \xi\phi^2)} \Big|_{\phi=\phi_i, q=q_i}, \\ r &= \frac{8(1 - 11\xi\phi^2)^2 D_l^{m-2(n+1)}}{9\kappa\phi^2 (1 + \xi\phi^2)} \Big|_{\phi=\phi_i, q=q_i}.\end{aligned}\quad (92)$$

Also, by using Eq. (26), the running of the spectral index is expressed as

$$\begin{aligned}\alpha_s &= \frac{242B_{\frac{1}{3}} \xi^2 A_{\frac{1}{3}} D_l^{-(n+1)} D_l^{-\frac{m}{2}-2(n+1)}}{27\kappa^2 \left(-13B_{\frac{1}{3}} A_{\frac{1}{3}} D_l^{-(n+1)} + A_{\frac{1}{3}}^2 D_l^{-(n+1)} + 12B_{\frac{1}{3}}^2 \right)^2} \\ &\quad \left[24B_{\frac{1}{3}} A_{\frac{1}{3}} D_l^{-(n+1)} (11D_l^{m/2} - 12D_l^{n+1}) + A_{\frac{1}{3}}^2 D_l^{-(n+1)} (78D_l^{n+1} - 143D_l^{m/2}) + 936B_{\frac{1}{3}}^2 D_l^{n+1} \right] \Big|_{q=q_i, N=N_i},\end{aligned}\quad (93)$$

with

$$A_{\frac{1}{3}} \equiv 1 - 11\xi\phi_f^2, \quad B_{\frac{1}{3}} \equiv e^{\frac{22\xi N D_l^{-(n+1)}}{3\kappa}}.\quad (94)$$

In FIG. 6, we present the theoretical predictions for the fractional monomial potential $V(\phi) \propto \phi^{1/3}$ under the influence of inverse-volume corrections. The left and right panels display the (n_s, r) and (n_s, α_s) planes, respectively, for various choices of the non-minimal coupling ξ . As before, we set the ambiguity parameters to $m = 0$ and $n = 0$, with $l = 3/4$ and an initial value $q_i = 100$. The theoretical curves, evaluated for an e-folding range between $N = 50$ and $N = 70$, are superimposed on the 1σ and 2σ confidence contours from Planck 2018 and the combined ACT data. To better understand the viable parameter space, FIG. 7 maps these observational bounds directly onto the (N, ξ) plane. This projection isolates the specific combinations of coupling strength and inflationary duration that successfully reproduce the observed CMB power spectra.

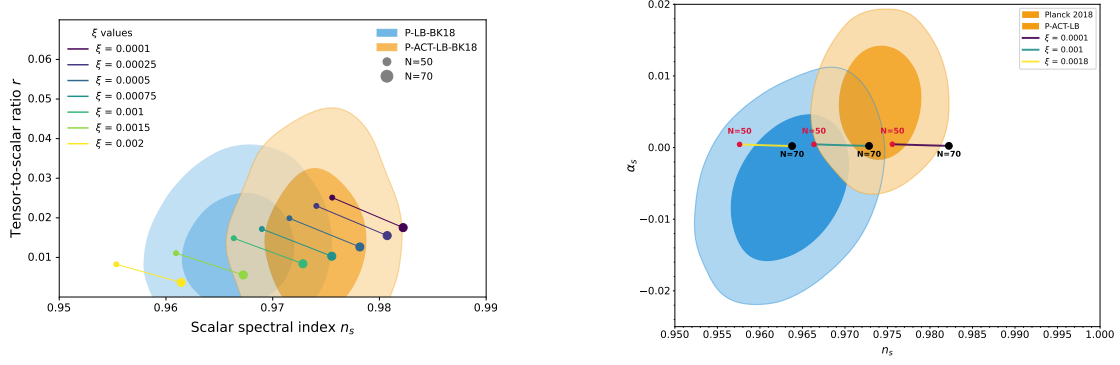


Figure 6: Inflationary predictions for $V(\phi) \propto \phi^{1/3}$ in LQC with inverse-volume corrections. Left panel shows r versus n_s and right panel shows α_s versus n_s for different non-minimal couplings ξ , with markers at $N = 50$ and $N = 70$. We fix the operator-ordering parameters $m = 0$, $n = 0$, the inverse-volume eigenvalue parameter $l = 3/4$, and the initial value $q_i = 100$.

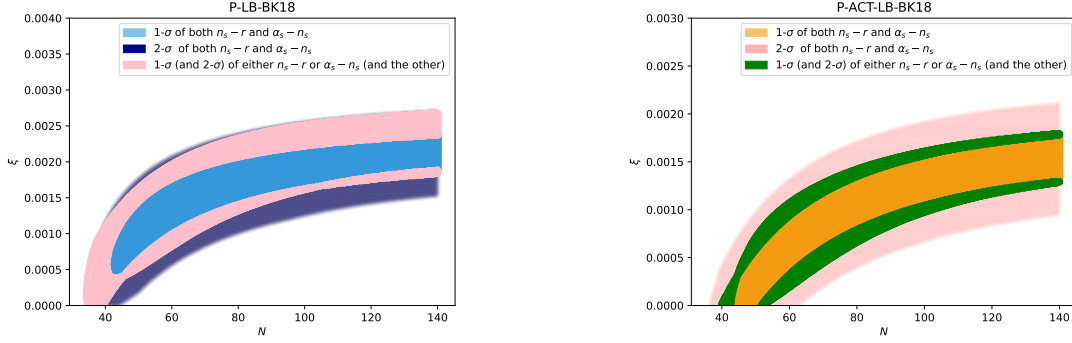


Figure 7: Allowed region in the (N, ξ) plane for the quartic potential $V(\phi) \propto \phi^{1/3}$ in LQC with inverse-volume corrections. The left panel uses P-LB-BK18 constraints and the right panel uses P-ACT-LB-BK18 constraints. We fix the operator-ordering parameters $m = 0$ and $n = 0$, the inverse-volume eigenvalue parameter $l = 3/4$, and the initial value $q_i = 100$.

5.1.2. $V(\phi) = \lambda\phi^{2/3}$

For the fractional monomial potential $V(\phi) = \lambda\phi^{2/3}$, we get the loop-corrected slow-roll parameters

$$\begin{aligned}\delta_X &= \frac{2(1 - 5\xi\phi^2)^2 D_l^{m-2(n+1)}}{9\kappa\phi^2(1 + \xi\phi^2)}, \\ \delta_U &= \frac{4\xi(5\xi\phi^2 - 1)D_l^{-(n+1)}}{3\kappa(1 + \xi\phi^2)}, \\ \epsilon &= -\frac{2(5\xi\phi^2 - 1)D_l^{-2(n+1)}[(1 - 5\xi\phi^2)D_l^m + 3\xi\phi^2 D_l^{n+1}]}{9\kappa\phi^2(1 + \xi\phi^2)}.\end{aligned}\quad (95)$$

From the condition $\epsilon = 1$ at the end of inflation, we have the final value of the inflaton

$$\phi_f^2 = \frac{4}{3\sqrt{9\kappa^2 + 36\kappa\xi + 4\xi^2 + 9\kappa + 14\xi}}.\quad (96)$$

The scalar power spectrum at the horizon crossing becomes

$$\mathcal{P}_s = D_l^{m+2(n+1)} \frac{3\kappa^3 \lambda \phi^{8/3}}{16\pi^2 (1 - 5\xi\phi^2)^2 (\xi\phi^2 + 1)} \Big|_{\phi=\phi_i, q=q_i},\quad (97)$$

which allows us to calculate $\lambda(N_*)$. Also, the corresponding spectral index and tensor-to-scalar ratio, evaluated at horizon exit ($\phi = \phi_i, q = q_i$), are given by

$$n_s - 1 = \frac{2 \left[D_l^{-\frac{m}{2}} (3\phi^2 (3\kappa(n+1)\delta_D (\xi\phi^2 + 1) - 14\xi) - 6) - 2(1 - 5\xi\phi^2)^2 D_l^{-(n+1)} \right]}{9\kappa\phi^2 (1 + \xi\phi^2)} \Big|_{\phi=\phi_i, q=q_i}, \quad (98)$$

$$r = \frac{32(1 - 5\xi\phi^2)^2 D_l^{m-2(n+1)}}{9\kappa\phi^2 (1 + \xi\phi^2)} \Big|_{\phi=\phi_i, q=q_i},$$

and the running of the scalar spectral index yields

$$\alpha_s = \frac{400B_{\frac{2}{3}}\xi^2 A_{\frac{2}{3}}^{D_l^{-(n+1)}} D_l^{-\frac{m}{2}-(n+1)}}{27\kappa^2 \left[B_{\frac{2}{3}} A_{\frac{2}{3}}^{D_l^{-(n+1)}} \left(B_{\frac{2}{3}} A_{\frac{2}{3}}^{D_l^{-(n+1)}} - 7 \right) + 6 \right]^2} \left[-12B_{\frac{2}{3}} A_{\frac{2}{3}}^{D_l^{-n-1}} (5D_l^{m/2} - 6D_l^{n+1}) \right. \\ \left. + 7B_{\frac{2}{3}}^2 A_{\frac{2}{3}}^{2D_l^{-(n+1)}} (5D_l^{m/2} - 3D_l^{n+1}) - 126D_l^{n+1} \right] \Big|_{q=q_i, N=N_i}, \quad (99)$$

where we defined

$$A_{\frac{2}{3}} \equiv 1 - 5\xi\phi_i^2, \quad B_{\frac{2}{3}} \equiv e^{\frac{20\xi N D_l^{-(n+1)}}{3\kappa}}. \quad (100)$$

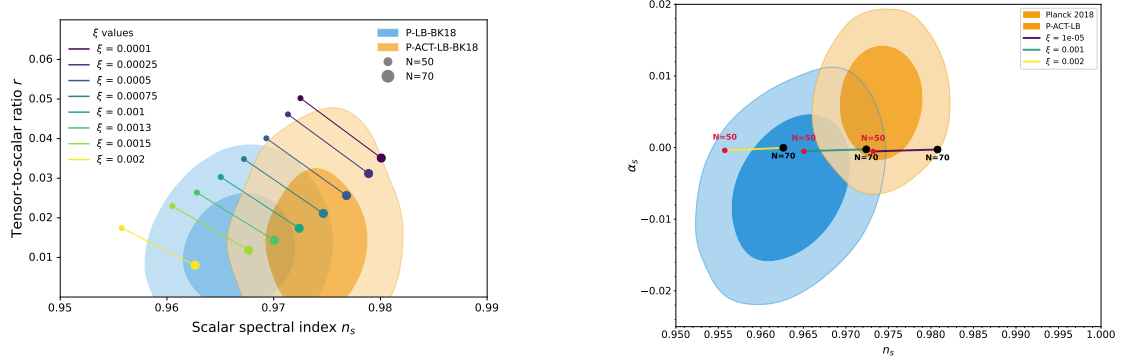


Figure 8: Inflationary predictions for $V(\phi) \propto \phi^{2/3}$ in LQC with inverse-volume corrections. Left panel shows r versus n_s and right panel shows α_s versus n_s for different non-minimal couplings ξ , with markers at $N = 50$ and $N = 70$. We fix the operator-ordering parameters $m = 0, n = 0$, the inverse-volume eigenvalue parameter $l = 3/4$, and the initial value $q_i = 100$.

The corresponding results for the $V(\phi) \propto \phi^{2/3}$ potential are illustrated in FIG. 8. Here again, we plot the predicted pairs of (n_s, r) and (n_s, α_s) against the background constraints, maintaining the same LQC parameter choices ($m = n = 0, l = 3/4$, and $q_i = 100$). The markers on the curves denote the standard window of 50 to 70 e-folds. Following the same procedure as in the previous cases, we then constrain the underlying model parameters by filtering the allowed points. The outcome is displayed in FIG. 9, which highlights the region in the (N, ξ) parameter space where the model remains fully consistent with both the scalar tilt and the bounds on the running and tensor modes.

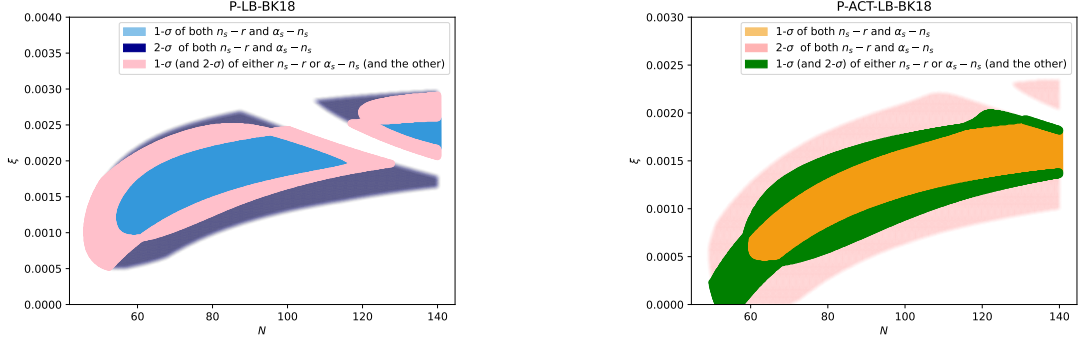


Figure 9: Allowed region in the (N, ξ) plane for the quartic potential $V(\phi) \propto \phi^{2/3}$ in LQC with inverse-volume corrections. The left panel uses P-LB-BK18 constraints and the right panel uses P-ACT-LB-BK18 constraints. We fix the operator-ordering parameters $m = 0$ and $n = 0$, the inverse-volume eigenvalue parameter $l = 3/4$, and the initial value $q_i = 100$.

$$(\eta_s)_{LQ} = 1.$$

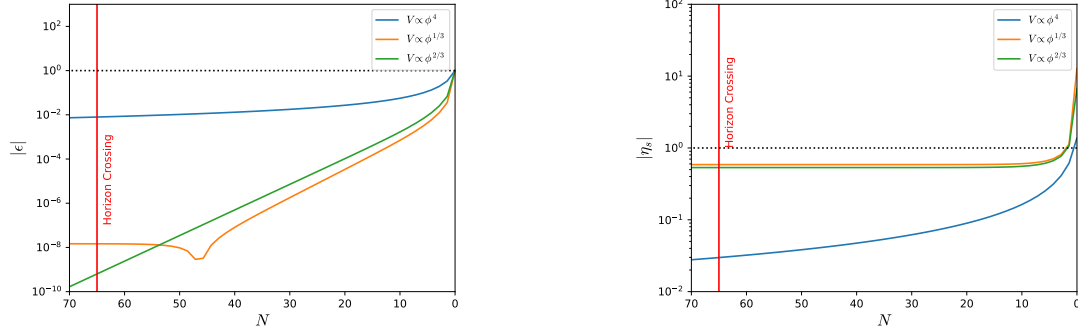


Figure 10: Evolution of slow-roll parameters with the number of e-folds N with $l = 3/4$ and $q_i = 100$. The dotted lines represent $\epsilon_{LQ} = 1$ and $(\eta_s)_{LQ} = 1$.

To explicitly verify the internal consistency of our approximation, we must track the dynamical evolution of the LQC-modified slow-roll parameters throughout the expansion. The left and right panels of FIG. 10 illustrate the behavior of $|\epsilon_{LQ}|$ and $|(\eta_s)_{LQ}|$, respectively, as functions of the e-folding number N . Deep in the inflationary regime, both parameters remain safely below unity, which guarantees a sustained quasi-de Sitter expansion. As the scalar field rolls toward the minimum of its effective potential, its kinetic energy gradually increases until the slow-roll conditions are no longer satisfied. This natural termination of slow-roll inflation is marked in the plots by the horizontal dotted lines at $\epsilon_{LQ} = 1$ and

5.2. Probability of inflation

5.2.1. $V(\phi) = \lambda\phi^{1/3}$

For this potential, under the slow-roll approximation, one finds

$$\frac{d\phi}{dN} = \frac{(11\xi\phi^2 - 1)D_l^{n+1}}{3\kappa\phi}. \quad (101)$$

Thus, the number of e -folds is computed as

$$N = \frac{3\kappa \log\left(\frac{11\xi\phi^2 - 1}{22\xi}\right) D_l^{-(n+1)}}{22\xi} \Bigg|_{\phi=\phi_i}^{\phi=\phi_f}. \quad (102)$$

We obtain the probability of inflation to be

$$\mathcal{P} \propto 2a_{\text{pl}}^3 q^{3/2} \sqrt{\frac{\lambda}{3\kappa}} \left[\sqrt{(\xi\phi_i^2 + 1)\phi_i^{1/3} D_l(q_i)^m} - \sqrt{(\xi\phi_f^2 + 1)\phi_f^{1/3}} \right], \quad (103)$$

where we have considered $D_l(q_f) = 1$.

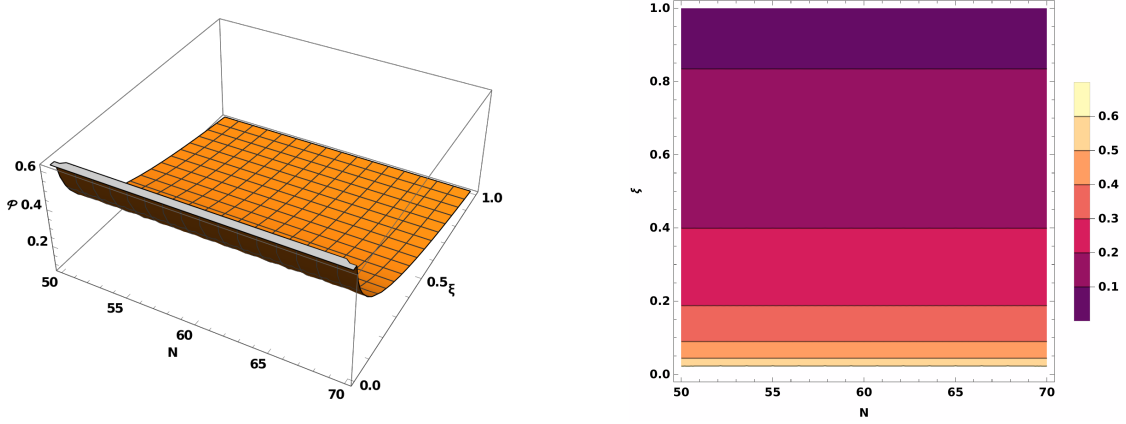


Figure 11: Effect of the non-minimal coupling ξ on the probability of inflation \mathcal{P} for the string-inspired fractional monomial potential $V(\phi) = \lambda\phi^{1/3}$, with $M_{\text{pl}}^{-11/3}\lambda \simeq 1.81 \times 10^{-10}$ inferred from the scalar power-spectrum amplitude $\mathcal{P}_s = 2.141 \times 10^{-9}$ Akrami et al. (2020). The left panel shows the surface $\mathcal{P}(N, \xi)$ and the right panel shows the corresponding contour map. We fix the inverse-volume eigenvalue parameter to $l = 3/4$ and the initial value to $q_i = 100$.

Following the same measure-theoretic approach, we calculate the probability of sufficient inflation for the fractional monomial potential $V(\phi) \propto \phi^{1/3}$. FIG. 11 maps the probability across the (N, ξ) plane, utilizing a 3D surface plot on the left and a contour projection on the right. For this evaluation, λ is fixed to satisfy the scalar power spectrum normalization. In stark contrast to the quartic case, the phase-space volume of favorable initial conditions for this fractional potential actually decreases as the non-minimal coupling grows. Although the axes are scaled to show a wide theoretical landscape spanning $\xi \in (0, 1)$ up to $N = 70$ ($M_{\text{pl}}^2 = 1$), the actual physical regime that simultaneously yields a high probability of inflation and remains consistent with precision cosmological data occupies an extremely narrow strip of the configured parameter space.

5.2.2. $V(\phi) = \lambda\phi^{2/3}$

Under the slow-roll approximation, we obtain

$$\frac{d\phi}{dN} = \frac{2(5\xi\phi^2 - 1)D_l^{n+1}}{3\kappa\phi}. \quad (104)$$

So, the number of e -folds can be computed as

$$N = \frac{3\kappa \log(5\xi\phi^2 - 1) D_l^{-(n+1)}}{20\xi} \Bigg|_{\phi=\phi_i}^{\phi=\phi_f}. \quad (105)$$

Hence, by using (70), we get the Probability

$$\mathcal{P} \propto 2a_{\text{pl}}^3 q^{3/2} \sqrt{\frac{\lambda}{3\kappa}} \left[\sqrt{(\xi\phi_i^2 + 1)\phi_i^{2/3} D_l(q_i)^m} - \sqrt{(\xi\phi_f^2 + 1)\phi_f^{2/3}} \right]. \quad (106)$$

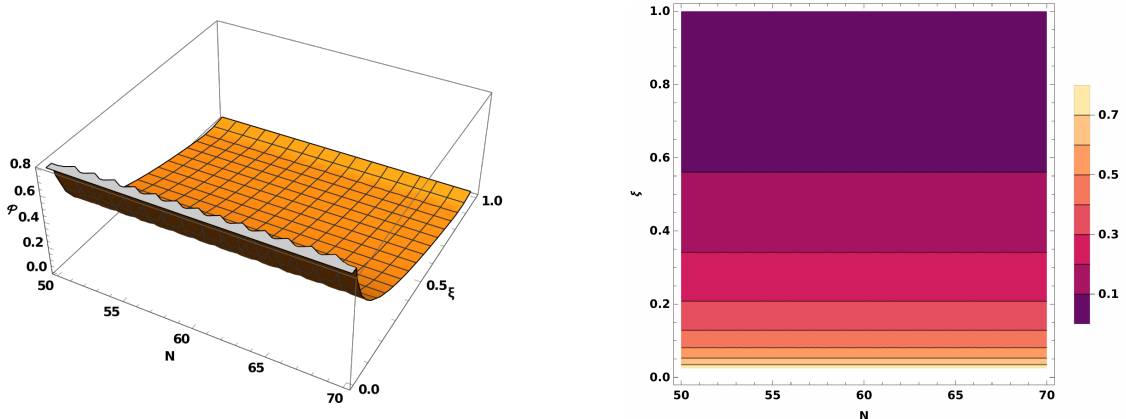


Figure 12: Effect of the non-minimal coupling ξ on the probability of inflation \mathcal{P} for the string-inspired fractional monomial potential $V(\phi) = \lambda\phi^{2/3}$, with $M_{pl}^{-10/3}\lambda \simeq 7.1 \times 10^{-10}$ inferred from the scalar power-spectrum amplitude $\mathcal{P}_s = 2.141 \times 10^{-9}$ Akrami et al. (2020). The left panel shows the surface $\mathcal{P}(N, \xi)$ and the right panel shows the corresponding contour map. We fix the inverse-volume eigenvalue parameter to $l = 3/4$ and the initial value to $q_i = 100$.

Finally, we present the phase-space probability distributions for the $V(\phi) \propto \phi^{2/3}$ potential. As in the preceding analyses, the 3D and contour plots in FIG. 12 demonstrate how the non-minimal coupling ξ and the total number of e-folds N influence the measure of favorable initial conditions, assuming a fixed λ calibrated by the primordial power spectrum. Similar to the $p = 1/3$ scenario, we observe an inverse relationship between the coupling strength and the probability of inflation, with larger values of ξ suppressing the likelihood of a sufficiently long slow-roll phase. We again plot this distribution over the wide macroscopic intervals $\xi \in (0, 1)$ and $N \in (0, 70)$ (with $M_{pl}^2 = 1$) to clearly display the overall functional behavior of the Liouville measure. Nevertheless, one must keep in mind that the parameter configurations capable of surviving the stringent observational cuts from Planck and ACT represent only a very small fraction of the total parameter space visualized here.

The results summarized in TABLE 1 illustrate how inverse-volume corrections map onto the precision constraints of modern cosmology across three distinct potentials: $V(\phi) \propto \phi^4$, $\phi^{1/3}$, and $\phi^{2/3}$. By tracking the slow-roll parameters at $N = 60, 65$, and 70 e-folds, we observe that the non-minimal coupling ξ is the critical parameter governing observational viability. For the Higgs-like quartic potential, standard LQC dynamics yield an unacceptably large tensor-to-scalar ratio; however, values of $\xi \approx 0.04$ successfully suppress r and tune the scalar tilt n_s into excellent 1σ agreement with the combined Planck and ACT DR6 data. In contrast, the string-inspired fractional monomial potentials naturally predict lower tensor contributions, thus requiring much smaller non-minimal couplings ($\xi \sim 0.001$) to achieve the optimal (n_s, r) and (n_s, α_s) fit. Across all three models, varying ξ effectively acts to tilt the primordial spectrum and modulate its running, establishing a very narrow phenomenological window within which LQC-corrected slow-roll trajectories accurately reproduce the observed universe.

Table 1: Predicted inflationary observables (n_s, r, α_s) and self-coupling λ for the ϕ^4 , $\phi^{1/3}$, and $\phi^{2/3}$ potentials with LQC inverse-volume corrections. Results are evaluated at $N = 60, 65$, and 70 e-folds for varying non-minimal coupling ξ . Colors denote consistency with Planck 2018 and ACT DR6 constraints in the (n_s, r) and (n_s, α_s) planes: ■ ($\leq 1\sigma$), ■ ($\leq 2\sigma$), and ■ ($> 2\sigma$). Highlighted ξ values indicate the optimal fit for each potential.

$V(\phi)$	ξ	N	n_s	r	α_s	λ	P – LB – BK18		P – ACT – LB – BK18	
							$n_s - r$	$n_s - \alpha_s$	$n_s - r$	$n_s - \alpha_s$
$\lambda\phi^4$	0.01	60	0.964	0.045	0.001	2.06×10^{-13}				
		65	0.967	0.039	0.001	1.73×10^{-13}				
		70	0.97	0.034	0	1.48×10^{-13}				
	0.04	60	0.966	0.013	0.001	7.19×10^{-13}				
		65	0.969	0.011	0	6.12×10^{-13}				
		70	0.971	0.01	0	5.27×10^{-13}				
	0.07	60	0.967	0.007	0.001	1.23×10^{-12}				
		65	0.969	0.006	0	1.05×10^{-12}				
		70	0.971	0.006	0	9.06×10^{-13}				
$\lambda\phi^{1/3}$	0.0005	60	0.975	0.016	0	2.18×10^{-10}				
		65	0.977	0.014	0	2.51×10^{-10}				
		70	0.978	0.013	0	2.25×10^{-10}				
	0.001	60	0.97	0.011	0	2.08×10^{-10}				
		65	0.972	0.01	0	1.80×10^{-10}				
		70	0.973	0.008	0	1.57×10^{-10}				
	0.0015	60	0.965	0.008	0	1.52×10^{-10}				
		65	0.966	0.007	0	1.28×10^{-10}				
		70	0.967	0.006	0	1.09×10^{-10}				
$\lambda\phi^{2/3}$	0.0005	60	0.974	0.032	0	7.96×10^{-10}				
		65	0.975	0.028	0	7.15×10^{-10}				
		70	0.977	0.026	0	6.47×10^{-10}				
	0.001	60	0.969	0.023	0	7.87×10^{-10}				
		65	0.971	0.02	0	7.07×10^{-10}				
		70	0.972	0.017	0	6.41×10^{-10}				
	0.0015	60	0.965	0.016	0	7.88×10^{-10}				
		65	0.966	0.014	0	7.10×10^{-10}				
		70	0.968	0.012	0	6.46×10^{-10}				

6. Discussion and Conclusion

In this work, we investigated slow-roll inflation driven by a scalar field non-minimally coupled to gravity within the effective framework of Loop Quantum Cosmology (LQC), incorporating inverse-volume corrections. For the two classes of potentials considered here, a Higgs-like quartic potential ($V \propto \phi^4$) and string-inspired fractional monomial potentials ($V \propto \phi^p$ with $p < 1$), we computed the inflationary observables in the inverse-volume-corrected dynamics in the presence of non-minimal coupling and confronted the resulting predictions with the latest observational constraints. We then quantified the probability of achieving sufficient inflation by constructing the canonical Liouville measure on the effective phase space and evaluating the fraction of post-bounce trajectories that yield $N \geq N_*$.

Our analysis shows that introducing a non-minimal coupling parameter ξ significantly enlarges the phase space volume of initial conditions that lead to sufficient inflation, compared to the minimally coupled case. This attractor-like

behavior saturates as the coupling strength increases, suggesting that non-minimal coupling renders inflation a generic outcome in these models within the LQC context. These results are particularly relevant in light of recent observational data. The Atacama Cosmology Telescope (ACT) DR6 and DESI analyses have indicated a preference for a scalar spectral index n_s slightly higher than the Planck 2018 best-fit value, and the running $\alpha_s \equiv dn_s/d \ln k$ provides an additional discriminator among viable scenarios. We find that, within the inverse-volume-corrected effective LQC dynamics considered here, the non-minimally coupled fractional monomial potentials and the non-minimally coupled Higgs-like quartic model naturally fall in the preferred region of the (n_s, r) plane, while the LQC bounce ensures the resolution of the initial singularity.

To connect our theoretical results on the probability of sufficient inflation with observations, we compare the parameter region where this probability is enhanced with the values of the non-minimal coupling ξ that are consistent with current CMB constraints on (n_s, r, α_s) . For the Higgs-like quartic potential $V \propto \phi^4$, viable fits typically require $\xi = \mathcal{O}(10^{-2})$, with ACT-based combinations favoring values toward the upper end of this range. By contrast, for fractional monomial potentials $V \propto \phi^p$ with $p < 1$ (e.g., $p = 1/3$ and $p = 2/3$), the preferred couplings are smaller, typically $\xi = \mathcal{O}(10^{-3})$, and can extend down to $\mathcal{O}(10^{-4})$ depending on the dataset and confidence level. Overall, the probability-enhanced region identified in our analysis overlaps with the order-of-magnitude values of ξ that remain compatible with current observational bounds for both classes of non-minimally coupled potentials.

A central contribution of this work is to jointly assess the effects of non-minimal coupling and inverse-volume corrections on the slow-roll dynamics and the probabilistic realization of inflation, going beyond most existing analyses in the literature that consider these ingredients separately. In particular, we find that introducing the non-minimal coupling shifts the inverse-volume-corrected predictions toward values of (n_s, r, α_s) that are more consistent with the ACT-preferred region, while simultaneously enlarging the phase-space measure of trajectories that yield sufficient inflation. Moreover, in the presence of inverse-volume corrections, the non-minimal coupling cannot, in general, be removed by field redefinitions [Bojowald and Kagan \(2006\)](#); [Han \(2019\)](#); [Artymowski et al. \(2013\)](#), and therefore constitutes a physical ingredient of the effective dynamics, not merely a parametrization choice.

It is worth emphasizing the domain of validity of our effective treatment. We focused on inverse-volume corrections and worked in the regime where the effective description is reliable. Quantization ambiguities associated with these corrections, encoded in the parameters controlling inverse-volume effects and in operator-ordering choices, can affect quantitative predictions. In particular, such ambiguities may shift the detailed numerical values of the observables and the inferred probability, although the qualitative trend of an enhancement followed by saturation of the probability for $N \geq N_\star$ as ξ increases remains stable across the representative ranges explored.

Our probability should be interpreted as a notion of typicality induced by the canonical Liouville measure on the effective constraint surface after gauge fixing. The enhancement with ξ reflects a nontrivial reweighting of the set of solutions. The non-minimal coupling changes the measure density on the transverse section used to evaluate the probability flux, thereby assigning greater weight to post-bounce trajectories that naturally converge to slow roll. This provides a dynamical explanation for why inflation becomes more generic in the non-minimally coupled case, beyond a mere shift of the slow-roll parameters.

Several extensions follow naturally from this work. A first step is to study the combined impact of holonomy and inverse-volume corrections in the presence of non-minimal coupling, allowing the bounce and the onset of inflation to be treated within unified effective dynamics. It would also be valuable to refine the perturbation analysis by tracking the evolution of modes across the pre-inflationary transition region, where LQC corrections may leave characteristic imprints and where the mapping between k and horizon crossing can be altered. Finally, incorporating reheating-consistent relations between N_\star and post-inflationary expansion would enable a tighter confrontation with current and forthcoming data, particularly through constraints on the running and tensor modes.

7. Acknowledgments

We thank the COSMOGRAV-UTA group for their continuous support and stimulating research environment. R.R. is particularly grateful to Orestis Sarrao for valuable discussions and Nitesh Kumar for providing the data and code used in this work. R.R. acknowledges financial support from the PhD fellowship of the UTA-ULS-UV consortium and Fondecyt Regular N°1220065.

Appendix A. Measure

Appendix A.1. Construction

Before defining the measure, we should expect the measure to satisfy three basic conditions:

1. It must be positive.
2. It must be independent of the parameters chosen. The measure will be a property of the model, not the initial condition of the parameter.
3. It must respect the symmetry of the space or the solution without introducing extra ad hoc structure.

Let us consider a system containing a finite number of variables and satisfying an ordinary differential equation with respect to the independent parameter “time”. We consider the evolution of the system as a flow in N -dimensional manifold θ . Each trajectory of the flow represents a unique model of inflation. Now we can define a hypersurface Σ intersecting the flow transversely in a $(N - 1)$ -surface S . We define a measure ν appropriate to the hypersurface to attach a weight $\mu(B)$ for each trajectory B [Gibbons et al. \(1987\)](#):

$$\mu(B) = \int_S \nu. \quad (\text{A.1})$$

Condition - 1 restricts $\mu(B) \geq 0$.

Condition - 2 removes the dependency of the measure on the chosen hypersurface.

If we consider another hypersurface Σ' with intersection S' , we will have the same measure

$$\mu(B) = \int_{S'} \nu. \quad (\text{A.2})$$

Now, regarding the differential flow, we may consider S' as some Lie transported version of S along the tangent vector to the orbit, V . The invariance yields the condition

$$\mathfrak{L}_{fV} \nu = 0, \quad (\text{A.3})$$

for an arbitrary function f .

Now we focus on the phase space dynamics. The system is described by the evolution in a $2n$ -dimensional phase space Γ_n . The evolution of the system is given by the $2n$ first-order evolution equations

$$\frac{dq^i}{dt} = \frac{\partial H(p, q)}{\partial p_i}, \quad \frac{dp^i}{dt} = -\frac{\partial H(p, q)}{\partial q_i}. \quad (\text{A.4})$$

The integral curves form the Hamiltonian phase flow along the tangent direction

$$X_H = \frac{\partial H(p, q)}{\partial p_i} \frac{\partial}{\partial q_i} - \frac{\partial H(p, q)}{\partial q_i} \frac{\partial}{\partial p_i}. \quad (\text{A.5})$$

As expected, the Hamiltonian remains invariant under the transportation along X_H

$$\mathfrak{L}_{X_H} H(p, q) = 0. \quad (\text{A.6})$$

To work with more general approach, it is better to get rid of the coordinates. We constrain the dynamics to be confined within the hypersurface θ in Γ_n with $H(p, q) = \text{constant}$. Within θ , we chose a $(2n - 2)$ -dimensional hypersurface Γ_{n-1} , transverse to the Hamiltonian flow. To connect these spaces, we define the embedding of the manifolds through push-forward mapping $\iota_1 : \theta \rightarrow \Gamma_n$, $\iota_2 : \Gamma_{n-1} \rightarrow \theta$. As Γ_n is even dimensional, we have a natural symplectic structure ω_n . The closed non-degenerate differential 2-form ω_n is preserved by the Hamiltonian phase flow

$$\mathfrak{L}_{X_H} \omega_n = 0. \quad (\text{A.7})$$

Following Darboux’s theorem [Arnold \(1989\)](#), there must exist some local coordinates (P_i, Q^i) such that ω_n takes the form

$$\omega_n = dP_i \wedge dQ^i. \quad (\text{A.8})$$

If we introduce $P_1 = H(p, q)$ and $Q^1 = t$, we can write

$$\omega_n = dH \wedge dt + \omega_{n-1}, \quad (\text{A.9})$$

where ω_{n-1} is the symplectic structure in Γ_{n-1} .

Now we can define the pull-back of ω_n from Γ_n to θ

$$\iota_1^* \omega_n = 0 \wedge dt + \omega_{n-1}, \quad (\text{A.10})$$

and pull-back onto Γ_{n-1} is

$$\iota_2^* \iota_1^* \omega_n = \omega_{n-1}. \quad (\text{A.11})$$

Hence, we have the natural Liouville measure on Γ_n and Γ_{n-1} , respectively [Gibbons et al. \(1987\)](#)

$$\Omega_n = (-1)^{n(n-1)/2} (\omega_n)^n \quad (\text{A.12})$$

$$\Omega_{n-1} = (-1)^{(n-1)(n-2)/2} (\omega_{n-1})^{n-1}. \quad (\text{A.13})$$

This measure already satisfies the conditions (1) and (3). We can check the condition (2) through the Cartan identity

$$\mathfrak{L}_{fX_H}(\iota_1^* \omega_n) = fX_H \lrcorner d(\iota_1^* \omega_n) + d(fX_H \lrcorner \iota_1^* \omega_n). \quad (\text{A.14})$$

where the symbol \lrcorner denotes the interior product (or contraction). This operation inserts the vector field fX_H into the first argument of the differential form, effectively mapping a k -form to a $(k-1)$ -form. Since ω_n is a closed form, the exterior derivative d and the pull-back commute, yielding $d(\iota_1^* \omega_n) = \iota_1^* d\omega_n = 0$. We have $fX_H = f \partial/\partial Q^1$ in the Darboux coordinate. Thus, $fX_H \lrcorner \iota_1^* \omega_n = 0$. Finally, we get the condition (2) as

$$\mathfrak{L}_{fX_H}(\iota_1^* \omega_n) = 0. \quad (\text{A.15})$$

Appendix A.2. Liouville Measures and Magnetic Flux

Though the natural measure Ω provides a valid measurement for the probability of inflation, it diverges due to the inclusion of infinitely many almost flat universes [Gibbons et al. \(1987\)](#). Gibbons and Turok [Gibbons and Turok \(2008\)](#) have defined an alternative measure based on the properties of a divergence-less field to describe the set of distinct dynamical trajectories or, equivalently, the set of classical initial conditions giving distinct histories. This new measure identifies all the nearly flat universes as the same, whose negligible differences cannot be detected from the observations.

We can identify the measure (A.12) with the flux of some divergence-less field, analogous to a ‘‘magnetic field’’. In general coordinates on phase space, we have the symplectic form [Gibbons and Turok \(2008\)](#)

$$\omega_{\mu\nu} = -\omega_{\nu\mu}, \quad (\text{A.16})$$

where $\mu, \nu = 1, 2, 3, \dots, 2n$, and $\det[\omega] \neq 0$. As ω is closed ($d\omega = 0$), we must have

$$d_{[\mu} \omega_{\nu\tau]} = 0. \quad (\text{A.17})$$

The Hamiltonian equation is given by [Gibbons and Turok \(2008\)](#)

$$V^\mu = \omega^{\mu\nu} \partial_\nu \mathcal{H}, \quad (\text{A.18})$$

where $V^\mu \equiv (dx^\mu/dt)$ is the velocity in the phase space. We can write $\omega_{\mu\nu} V^\mu = \partial_\nu \mathcal{H}$, or equivalently

$$V^\mu \partial_\mu \mathcal{H} = 0. \quad (\text{A.19})$$

Hence, the flow V^μ lies on the hypersurface $\mathcal{H} = \text{constant}$.

If we choose the coordinate $x^{2n} = \mathcal{H}$, the closure condition is restricted to the spatial indices

$$d_{[a} \omega_{bc]} = 0, \quad (\text{A.20})$$

and

$$V^{2n} = 0, \quad (\text{A.21})$$

with $a, b = 1, 2, 3, \dots, 2n - 1$.

As the Hamiltonian is conserved, i.e $\partial_t \mathcal{H} = 0$, we must have

$$V^a \omega_{ab} = 0. \quad (\text{A.22})$$

As ω is closed, one can define a divergence-less field (analogous to a magnetic field)

$$B_a \equiv \frac{1}{2} \epsilon_{abc} \omega_{bc}, \quad (\text{A.23})$$

with

$$\partial_a B_a = 0. \quad (\text{A.24})$$

Hence,

$$\epsilon_{abc} B_b V_c = 0, \quad (\text{A.25})$$

that is to say $\mathbf{V} \parallel \mathbf{B}$.

Fundamental considerations from the divergence theorem show that the flux through a fixed surface does not change under deformations that preserve its boundary [Gibbons and Turok \(2008\)](#). Moreover, propagating the surface forward with the flow also leaves the flux unchanged.

For any phase space, we have a symplectic form [Gibbons et al. \(1987\)](#)

$$\Omega = \sum_{i=1}^k dP_i \wedge dQ^i, \quad (\text{A.26})$$

where Q_i and P_i are the dynamical degrees of freedom and their conjugate momenta.

The phase space also contains a closed symplectic form

$$\omega = \sum_{i=1}^{k-1} dP_i \wedge dQ^i, \quad (\text{A.27})$$

with the relation

$$\Omega = \omega + d\mathcal{H} \wedge dt, \quad (\text{A.28})$$

and then

$$\omega = \Omega \Big|_{\mathcal{H}=0}. \quad (\text{A.29})$$

Hence, these two symplectic forms are connected to each other through Hamiltonian constraint.

This construction can be extended to the effective Hamiltonian $\langle \widehat{\mathcal{H}}_{LQ} \rangle$:

$$\omega = \Omega \Big|_{\langle \widehat{\mathcal{H}}_{LQ} \rangle = 0} \quad (\text{A.30})$$

From the symplectic form, we can define a divergence-less field [Gibbons and Turok \(2008\)](#)

$$B_a = \frac{1}{2} \epsilon_{abc} \omega_{bc}. \quad (\text{A.31})$$

The field \mathbf{B} defines the flow of trajectories across surfaces in the phase space. Due to the divergence-less nature of the field \mathbf{B} , we can define an associated vector potential $\mathbf{B} = d\mathbf{A}$. Hence, we can define a measure using Stokes' theorem [Schiffin and Wald \(2012\)](#)

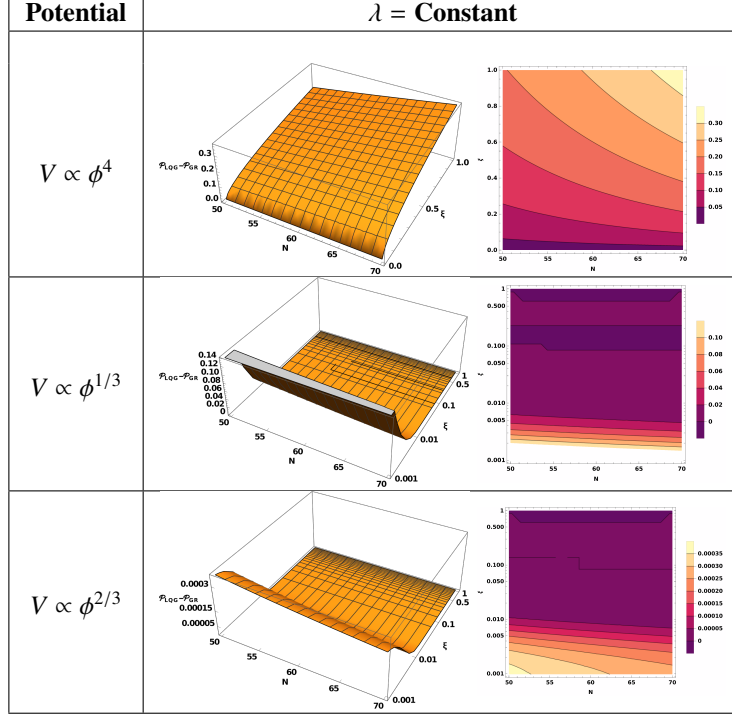
$$\mathcal{N} = \int \mathbf{B} \cdot d\mathbf{S} = \oint \mathbf{A} \cdot d\mathbf{l}, \quad (\text{A.32})$$

where \mathbf{S} is an open surface and $\mathbf{l} = \partial\mathbf{S}$ is the boundary of \mathbf{S} . To avoid over-counting, the surface \mathbf{S} is defined in such a way that the orbits cross through the surface only once.

The quantity \mathcal{N} measures the number of trajectories crossing the surface \mathbf{S} (or some equivalent surface) bounded by $\partial\mathbf{S}$.

Appendix B. Difference of Probability between the Inverse-Volume Corrected and the Classical

Table B.2: Change in Probability due to inverse-volume correction with $l = 3/4$ and $q_i = 100$. The values of self-coupling parameters λ are fixed according to the scalar power spectrum.



To explicitly isolate the impact of the quantum geometric modifications, this appendix compares the probability of inflation derived from the effective non-minimally coupled LQC dynamics against the standard classical General Relativity (GR) expectation. Table B.2 presents this comparison across all three studied potentials: $V(\phi) \propto \phi^4$, $\phi^{1/3}$, and $\phi^{2/3}$. For each model, we calculate the absolute difference between the inverse-volume corrected probability and the uncorrected classical probability, plotting the result as a function of the non-minimal coupling parameter ξ and the number of e-folds N . In these evaluations, the scale parameter λ is continuously fixed to satisfy the scalar power spectrum normalization, while the LQC parameters are set to $l = 3/4$ and the initial state to $q_i = 100$. The 3D surface plots and their corresponding contour maps clearly visualize the net topological effect of the loop quantum corrections, revealing exactly where in the parameter space the inverse-volume modifications enhance or suppress the phase-space volume of favorable initial conditions relative to the standard classical framework.

References

- Adame, A.G., et al. (DESI), 2025a. DESI 2024 III: baryon acoustic oscillations from galaxies and quasars. JCAP 04, 012. doi:[10.1088/1475-7516/2025/04/012](https://doi.org/10.1088/1475-7516/2025/04/012), [arXiv:2404.03000](https://arxiv.org/abs/2404.03000).
- Adame, A.G., et al. (DESI), 2025b. DESI 2024 VI: cosmological constraints from the measurements of baryon acoustic oscillations. JCAP 02, 021. doi:[10.1088/1475-7516/2025/02/021](https://doi.org/10.1088/1475-7516/2025/02/021), [arXiv:2404.03002](https://arxiv.org/abs/2404.03002).
- Agullo, I., Corichi, A., 2014. Loop Quantum Cosmology. Springer. pp. 809–839. doi:[10.1007/978-3-642-41992-8_39](https://doi.org/10.1007/978-3-642-41992-8_39), [arXiv:1302.3833](https://arxiv.org/abs/1302.3833).
- Akrami, Y., et al. (Planck), 2020. Planck 2018 results. X. Constraints on inflation. Astron. Astrophys. 641, A10. doi:[10.1051/0004-6361/201833887](https://doi.org/10.1051/0004-6361/201833887), [arXiv:1807.06211](https://arxiv.org/abs/1807.06211).

- Albrecht, A., Steinhardt, P.J., 1982. Cosmology for Grand Unified Theories with Radiatively Induced Symmetry Breaking. *Phys. Rev. Lett.* 48, 1220–1223. doi:[10.1103/PhysRevLett.48.1220](https://doi.org/10.1103/PhysRevLett.48.1220).
- Arnold, V.I., 1989. *Mathematical Methods of Classical Mechanics*. Graduate Texts in Mathematics, Springer. doi:[10.1007/978-1-4757-2063-1](https://doi.org/10.1007/978-1-4757-2063-1).
- Artymowski, M., Dapor, A., Pawłowski, T., 2013. Inflation from non-minimally coupled scalar field in loop quantum cosmology. *JCAP* 06, 010. doi:[10.1088/1475-7516/2013/06/010](https://doi.org/10.1088/1475-7516/2013/06/010), [arXiv:1207.4353](https://arxiv.org/abs/1207.4353).
- Ashtekar, A., 1986. New Variables for Classical and Quantum Gravity. *Phys. Rev. Lett.* 57, 2244–2247. doi:[10.1103/PhysRevLett.57.2244](https://doi.org/10.1103/PhysRevLett.57.2244).
- Ashtekar, A., 1987. New Hamiltonian Formulation of General Relativity. *Phys. Rev. D* 36, 1587–1602. doi:[10.1103/PhysRevD.36.1587](https://doi.org/10.1103/PhysRevD.36.1587).
- Ashtekar, A., Lewandowski, J., 2004. Background independent quantum gravity: A Status report. *Class. Quant. Grav.* 21, R53. doi:[10.1088/0264-9381/21/15/R01](https://doi.org/10.1088/0264-9381/21/15/R01), [arXiv:gr-qc/0404018](https://arxiv.org/abs/gr-qc/0404018).
- Ashtekar, A., Pawłowski, T., Singh, P., 2006. Quantum nature of the big bang. *Phys. Rev. Lett.* 96, 141301. doi:[10.1103/PhysRevLett.96.141301](https://doi.org/10.1103/PhysRevLett.96.141301), [arXiv:gr-qc/0602086](https://arxiv.org/abs/gr-qc/0602086).
- Ashtekar, A., Singh, P., 2011. Loop Quantum Cosmology: A Status Report. *Class. Quant. Grav.* 28, 213001. doi:[10.1088/0264-9381/28/21/213001](https://doi.org/10.1088/0264-9381/28/21/213001), [arXiv:1108.0893](https://arxiv.org/abs/1108.0893).
- Ashtekar, A., Sloan, D., 2011a. Loop quantum cosmology and slow roll inflation. *Phys. Lett. B* 694, 108–112. doi:[10.1016/j.physletb.2010.09.058](https://doi.org/10.1016/j.physletb.2010.09.058), [arXiv:0912.4093](https://arxiv.org/abs/0912.4093).
- Ashtekar, A., Sloan, D., 2011b. Probability of Inflation in Loop Quantum Cosmology. *Gen. Rel. Grav.* 43, 3619–3655. doi:[10.1007/s10714-011-1246-y](https://doi.org/10.1007/s10714-011-1246-y), [arXiv:1103.2475](https://arxiv.org/abs/1103.2475).
- Barboza, L.N., Graef, L.L., Ramos, R.O., 2020. Warm bounce in loop quantum cosmology and the prediction for the duration of inflation. *Phys. Rev. D* 102, 103521. doi:[10.1103/PhysRevD.102.103521](https://doi.org/10.1103/PhysRevD.102.103521), [arXiv:2009.13587](https://arxiv.org/abs/2009.13587).
- Bardeen, J.M., Steinhardt, P.J., Turner, M.S., 1983. Spontaneous Creation of Almost Scale - Free Density Perturbations in an Inflationary Universe. *Phys. Rev. D* 28, 679. doi:[10.1103/PhysRevD.28.679](https://doi.org/10.1103/PhysRevD.28.679).
- Baumann, D., McAllister, L., 2015. *Inflation and String Theory*. Cambridge Monographs on Mathematical Physics, Cambridge University Press. doi:[10.1017/CB09781316105733](https://doi.org/10.1017/CB09781316105733), [arXiv:1404.2601](https://arxiv.org/abs/1404.2601).
- Bedić, S., Vereshchagin, G., 2019. Probability of inflation in Loop Quantum Cosmology. *Phys. Rev. D* 99, 043512. doi:[10.1103/PhysRevD.99.043512](https://doi.org/10.1103/PhysRevD.99.043512), [arXiv:1807.06554](https://arxiv.org/abs/1807.06554).
- Bezrukov, F., Shaposhnikov, M., 2009. Standard Model Higgs boson mass from inflation: Two loop analysis. *JHEP* 07, 089. doi:[10.1088/1126-6708/2009/07/089](https://doi.org/10.1088/1126-6708/2009/07/089), [arXiv:0904.1537](https://arxiv.org/abs/0904.1537).
- Bezrukov, F.L., Shaposhnikov, M., 2008. The Standard Model Higgs boson as the inflaton. *Phys. Lett. B* 659, 703–706. doi:[10.1016/j.physletb.2007.11.072](https://doi.org/10.1016/j.physletb.2007.11.072), [arXiv:0710.3755](https://arxiv.org/abs/0710.3755).
- Birrell, N.D., Davies, P.C.W., 1982. *Quantum Fields in Curved Space*. Cambridge Monographs on Mathematical Physics, Cambridge University Press, Cambridge, UK. doi:[10.1017/CB09780511622632](https://doi.org/10.1017/CB09780511622632).
- Bojowald, M., 2001. Absence of singularity in loop quantum cosmology. *Phys. Rev. Lett.* 86, 5227–5230. doi:[10.1103/PhysRevLett.86.5227](https://doi.org/10.1103/PhysRevLett.86.5227), [arXiv:gr-qc/0102069](https://arxiv.org/abs/gr-qc/0102069).
- Bojowald, M., 2002a. Inflation from quantum geometry. *Phys. Rev. Lett.* 89, 261301. doi:[10.1103/PhysRevLett.89.261301](https://doi.org/10.1103/PhysRevLett.89.261301), [arXiv:gr-qc/0206054](https://arxiv.org/abs/gr-qc/0206054).
- Bojowald, M., 2002b. Quantization ambiguities in isotropic quantum geometry. *Class. Quant. Grav.* 19, 5113–5230. doi:[10.1088/0264-9381/19/20/306](https://doi.org/10.1088/0264-9381/19/20/306), [arXiv:gr-qc/0206053](https://arxiv.org/abs/gr-qc/0206053).

- Bojowald, M., 2004. Loop quantum cosmology: Recent progress. *Pramana* 63, 765–776. doi:[10.1007/BF02705198](https://doi.org/10.1007/BF02705198), [arXiv:gr-qc/0402053](https://arxiv.org/abs/gr-qc/0402053).
- Bojowald, M., 2005. Loop quantum cosmology. *Living Rev. Rel.* 8, 11. doi:[10.12942/lrr-2005-11](https://doi.org/10.12942/lrr-2005-11), [arXiv:gr-qc/0601085](https://arxiv.org/abs/gr-qc/0601085).
- Bojowald, M., 2007. Singularities and Quantum Gravity. *AIP Conf. Proc.* 910, 294–333. doi:[10.1063/1.2752483](https://doi.org/10.1063/1.2752483), [arXiv:gr-qc/0702144](https://arxiv.org/abs/gr-qc/0702144).
- Bojowald, M., Kagan, M., 2006. Loop cosmological implications of a non-minimally coupled scalar field. *Phys. Rev. D* 74, 044033. doi:[10.1103/PhysRevD.74.044033](https://doi.org/10.1103/PhysRevD.74.044033), [arXiv:gr-qc/0606082](https://arxiv.org/abs/gr-qc/0606082).
- Bojowald, M., Lidsey, J.E., Mulryne, D.J., Singh, P., Tavakol, R., 2004. Inflationary cosmology and quantization ambiguities in semiclassical loop quantum gravity. *Phys. Rev. D* 70, 043530. doi:[10.1103/PhysRevD.70.043530](https://doi.org/10.1103/PhysRevD.70.043530), [arXiv:gr-qc/0403106](https://arxiv.org/abs/gr-qc/0403106).
- Bojowald, M., Vandersloot, K., 2003. Loop quantum cosmology, boundary proposals, and inflation. *Phys. Rev. D* 67, 124023. doi:[10.1103/PhysRevD.67.124023](https://doi.org/10.1103/PhysRevD.67.124023), [arXiv:gr-qc/0303072](https://arxiv.org/abs/gr-qc/0303072).
- Brandenberger, R., 2016. Initial conditions for inflation — A short review. *Int. J. Mod. Phys. D* 26, 1740002. doi:[10.1142/S0218271817400028](https://doi.org/10.1142/S0218271817400028), [arXiv:1601.01918](https://arxiv.org/abs/1601.01918).
- Buchbinder, I.L., Odintsov, S.D., Shapiro, I.L., 1992. *Effective Action in Quantum Gravity*. IOP Publishing, Bristol. doi:[10.1201/9780203758922](https://doi.org/10.1201/9780203758922).
- Burgess, C.P., 2007. Introduction to Effective Field Theory. *Ann. Rev. Nucl. Part. Sci.* 57, 329–362. doi:[10.1146/annurev.nucl.56.080805.140508](https://doi.org/10.1146/annurev.nucl.56.080805.140508), [arXiv:hep-th/0701053](https://arxiv.org/abs/hep-th/0701053).
- Calabrese, E., et al. (Atacama Cosmology Telescope), 2025. The Atacama Cosmology Telescope: DR6 constraints on extended cosmological models. *JCAP* 11, 063. doi:[10.1088/1475-7516/2025/11/063](https://doi.org/10.1088/1475-7516/2025/11/063), [arXiv:2503.14454](https://arxiv.org/abs/2503.14454).
- Camphuis, E., et al. (SPT-3G), 2025. SPT-3G D1: CMB temperature and polarization power spectra and cosmology from 2019 and 2020 observations of the SPT-3G Main field. *arXiv preprint arXiv:2506.20707* [arXiv:2506.20707](https://arxiv.org/abs/2506.20707).
- Capozziello, S., De Laurentis, M., 2011. Extended Theories of Gravity. *Phys. Rept.* 509, 167–321. doi:[10.1016/j.physrep.2011.09.003](https://doi.org/10.1016/j.physrep.2011.09.003), [arXiv:1108.6266](https://arxiv.org/abs/1108.6266).
- Chen, L., Zhu, J.Y., 2015. Loop quantum cosmology: The horizon problem and the probability of inflation. *Phys. Rev. D* 92, 084063. doi:[10.1103/PhysRevD.92.084063](https://doi.org/10.1103/PhysRevD.92.084063), [arXiv:1510.03135](https://arxiv.org/abs/1510.03135).
- Cheung, C., Creminelli, P., Fitzpatrick, A.L., Kaplan, J., Senatore, L., 2008. The Effective Field Theory of Inflation. *JHEP* 03, 014. doi:[10.1088/1126-6708/2008/03/014](https://doi.org/10.1088/1126-6708/2008/03/014), [arXiv:0709.0293](https://arxiv.org/abs/0709.0293).
- Clifton, T., Ferreira, P.G., Padilla, A., Skordis, C., 2012. Modified Gravity and Cosmology. *Phys. Rept.* 513, 1–189. doi:[10.1016/j.physrep.2012.01.001](https://doi.org/10.1016/j.physrep.2012.01.001), [arXiv:1106.2476](https://arxiv.org/abs/1106.2476).
- Clough, K., Lim, E.A., DiNunno, B.S., Fischler, W., Flauger, R., Paban, S., 2017. Robustness of Inflation to Inhomogeneous Initial Conditions. *JCAP* 09, 025. doi:[10.1088/1475-7516/2017/09/025](https://doi.org/10.1088/1475-7516/2017/09/025), [arXiv:1608.04408](https://arxiv.org/abs/1608.04408).
- Copeland, E.J., Mulryne, D.J., Nunes, N.J., Shaeri, M., 2008. Super-inflation in Loop Quantum Cosmology. *Phys. Rev. D* 77, 023510. doi:[10.1103/PhysRevD.77.023510](https://doi.org/10.1103/PhysRevD.77.023510), [arXiv:0708.1261](https://arxiv.org/abs/0708.1261).
- De Felice, A., Tsujikawa, S., 2010. $f(R)$ theories. *Living Rev. Rel.* 13, 3. doi:[10.12942/lrr-2010-3](https://doi.org/10.12942/lrr-2010-3), [arXiv:1002.4928](https://arxiv.org/abs/1002.4928).
- De Felice, A., Tsujikawa, S., 2011. Inflationary non-Gaussianities in the most general second-order scalar-tensor theories. *Phys. Rev. D* 84, 083504. doi:[10.1103/PhysRevD.84.083504](https://doi.org/10.1103/PhysRevD.84.083504), [arXiv:1107.3917](https://arxiv.org/abs/1107.3917).

- De Felice, A., Tsujikawa, S., Elliston, J., Tavakol, R., 2011. Chaotic inflation in modified gravitational theories. JCAP 08, 021. doi:[10.1088/1475-7516/2011/08/021](https://doi.org/10.1088/1475-7516/2011/08/021), [arXiv:1105.4685](https://arxiv.org/abs/1105.4685).
- East, W.E., Kleban, M., Linde, A., Senatore, L., 2016. Beginning inflation in an inhomogeneous universe. JCAP 09, 010. doi:[10.1088/1475-7516/2016/09/010](https://doi.org/10.1088/1475-7516/2016/09/010), [arXiv:1511.05143](https://arxiv.org/abs/1511.05143).
- Ellis, J., Garcia, M.A.G., Olive, K.A., Verner, S., 2025. Constraints on Attractor Models of Inflation and Reheating from Planck, BICEP/Keck, ACT DR6, and SPT-3G Data. arXiv preprint [arXiv:2510.18656](https://arxiv.org/abs/2510.18656).
- Faraoni, V., Capozziello, S., 2011. Beyond Einstein Gravity: A Survey of Gravitational Theories for Cosmology and Astrophysics. Springer, Dordrecht. doi:[10.1007/978-94-007-0165-6](https://doi.org/10.1007/978-94-007-0165-6).
- Franciolini, G., Giudice, G.F., Racco, D., Riotto, A., 2019. Implications of the detection of primordial gravitational waves for the Standard Model. JCAP 05, 022. doi:[10.1088/1475-7516/2019/05/022](https://doi.org/10.1088/1475-7516/2019/05/022), [arXiv:1811.08118](https://arxiv.org/abs/1811.08118).
- Gambini, R., Pullin, J., 2011. A first course in loop quantum gravity. Oxford University Press, Oxford, New York. doi:[10.1093/acprof:oso/9780199590759.001.0001](https://doi.org/10.1093/acprof:oso/9780199590759.001.0001).
- Gao, Q., Qian, Y., Gong, Y., Yi, Z., 2025. Observational constraints on inflationary models with non-minimally derivative coupling by ACT. JCAP 08, 083. doi:[10.1088/1475-7516/2025/08/083](https://doi.org/10.1088/1475-7516/2025/08/083), [arXiv:2506.18456](https://arxiv.org/abs/2506.18456).
- Germani, C., Nelson, W., Sakellariadou, M., 2007. On the Onset of Inflation in Loop Quantum Cosmology. Phys. Rev. D 76, 043529. doi:[10.1103/PhysRevD.76.043529](https://doi.org/10.1103/PhysRevD.76.043529), [arXiv:gr-qc/0701172](https://arxiv.org/abs/gr-qc/0701172).
- Gialamas, I.D., Karam, A., Racioppi, A., Raidal, M., 2025. Has ACT measured radiative corrections to the tree-level Higgs-like inflation? Phys. Rev. D 112, 103544. doi:[10.1103/6fpc-67s1](https://doi.org/10.1103/6fpc-67s1), [arXiv:2504.06002](https://arxiv.org/abs/2504.06002).
- Gibbons, G.W., Hawking, S.W., Stewart, J.M., 1987. A Natural Measure on the Set of All Universes. Nucl. Phys. B 281, 736. doi:[10.1016/0550-3213\(87\)90425-1](https://doi.org/10.1016/0550-3213(87)90425-1).
- Gibbons, G.W., Turok, N., 2008. The Measure Problem in Cosmology. Phys. Rev. D 77, 063516. doi:[10.1103/PhysRevD.77.063516](https://doi.org/10.1103/PhysRevD.77.063516), [arXiv:hep-th/0609095](https://arxiv.org/abs/hep-th/0609095).
- Goldwirth, D.S., Piran, T., 1990. Inhomogeneity and the Onset of Inflation. Phys. Rev. Lett. 64, 2852–2855. doi:[10.1103/PhysRevLett.64.2852](https://doi.org/10.1103/PhysRevLett.64.2852).
- Graef, L.L., Ramos, R.O., 2018. Probability of Warm Inflation in Loop Quantum Cosmology. Phys. Rev. D 98, 023531. doi:[10.1103/PhysRevD.98.023531](https://doi.org/10.1103/PhysRevD.98.023531), [arXiv:1805.05985](https://arxiv.org/abs/1805.05985).
- Guth, A.H., 1981. The Inflationary Universe: A Possible Solution to the Horizon and Flatness Problems. Phys. Rev. D 23, 347–356. doi:[10.1103/PhysRevD.23.347](https://doi.org/10.1103/PhysRevD.23.347).
- Han, Y., 2019. Loop quantum cosmological dynamics of scalar-tensor theory in the Jordan frame. Phys. Rev. D 100, 123541. doi:[10.1103/PhysRevD.100.123541](https://doi.org/10.1103/PhysRevD.100.123541), [arXiv:1911.01128](https://arxiv.org/abs/1911.01128).
- Kalosh, R., Linde, A., 2025. On the present status of inflationary cosmology. Gen. Rel. Grav. 57, 135. doi:[10.1007/s10714-025-03470-6](https://doi.org/10.1007/s10714-025-03470-6), [arXiv:2505.13646](https://arxiv.org/abs/2505.13646).
- Kalosh, R., Linde, A., Roest, D., 2025. Atacama Cosmology Telescope, South Pole Telescope, and Chaotic Inflation. Phys. Rev. Lett. 135, 161001. doi:[10.1103/d6gn-78hn](https://doi.org/10.1103/d6gn-78hn), [arXiv:2503.21030](https://arxiv.org/abs/2503.21030).
- Kobayashi, T., 2019. Horndeski theory and beyond: a review. Rept. Prog. Phys. 82, 086901. doi:[10.1088/1361-6633/ab2429](https://doi.org/10.1088/1361-6633/ab2429), [arXiv:1901.07183](https://arxiv.org/abs/1901.07183).
- Kumar, N., Otalora, G., Reyes, R., Espinoza, B., Gonzalez-Espinoza, M., Saridakis, E.N., 2025. Higgs-like inflation in scalar-torsion $f(T, \phi)$ gravity in light of ACT-SPT-DESI constraints. arXiv preprint [arXiv:2512.24502](https://arxiv.org/abs/2512.24502).

- Leyva, Y., Leiva, C., Otalora, G., Saavedra, J., 2022. Inflation and primordial fluctuations in F(T) gravity's rainbow. *Phys. Rev. D* 105, 043523. doi:[10.1103/PhysRevD.105.043523](https://doi.org/10.1103/PhysRevD.105.043523), [arXiv:2111.07098](https://arxiv.org/abs/2111.07098).
- Leyva, Y., Otalora, G., 2023. Revisiting f(R) gravity's rainbow: Inflation and primordial fluctuations. *JCAP* 04, 030. doi:[10.1088/1475-7516/2023/04/030](https://doi.org/10.1088/1475-7516/2023/04/030), [arXiv:2206.09000](https://arxiv.org/abs/2206.09000).
- Li, B.F., Singh, P., 2024. *Loop Quantum Cosmology: Physics of Singularity Resolution and Its Implications*. Springer Nature Singapore, Singapore. pp. 3983–4037. URL: https://doi.org/10.1007/978-981-99-7681-2_102, doi:[10.1007/978-981-99-7681-2_102](https://doi.org/10.1007/978-981-99-7681-2_102), [arXiv:2304.05426](https://arxiv.org/abs/2304.05426).
- Liddle, A.R., Lyth, D.H., 2000. *Cosmological inflation and large scale structure*. Cambridge University Press. doi:[10.1017/CB09781139175180](https://doi.org/10.1017/CB09781139175180).
- Linde, A., 2018. On the problem of initial conditions for inflation. *Found. Phys.* 48, 1246–1260. doi:[10.1007/s10701-018-0177-9](https://doi.org/10.1007/s10701-018-0177-9), [arXiv:1710.04278](https://arxiv.org/abs/1710.04278).
- Linde, A.D., 1982. A New Inflationary Universe Scenario: A Possible Solution of the Horizon, Flatness, Homogeneity, Isotropy and Primordial Monopole Problems. *Phys. Lett. B* 108, 389–393. doi:[10.1016/0370-2693\(82\)91219-9](https://doi.org/10.1016/0370-2693(82)91219-9).
- López, M., Otalora, G., Videla, N., 2021. Chaotic inflation and reheating in generalized scalar-tensor gravity. *JCAP* 10, 021. doi:[10.1088/1475-7516/2021/10/021](https://doi.org/10.1088/1475-7516/2021/10/021), [arXiv:2107.07679](https://arxiv.org/abs/2107.07679).
- Louis, T., et al. (Atacama Cosmology Telescope), 2025. The Atacama Cosmology Telescope: DR6 power spectra, likelihoods and Λ CDM parameters. *JCAP* 11, 062. doi:[10.1088/1475-7516/2025/11/062](https://doi.org/10.1088/1475-7516/2025/11/062), [arXiv:2503.14452](https://arxiv.org/abs/2503.14452).
- Maity, S., 2025. ACT-ing on inflation: Implications of non bunch-Davies initial condition and reheating on single-field slow roll models. *Phys. Lett. B* 870, 139913. doi:[10.1016/j.physletb.2025.139913](https://doi.org/10.1016/j.physletb.2025.139913), [arXiv:2505.10534](https://arxiv.org/abs/2505.10534).
- Martin, J., Ringeval, C., Vennin, V., 2014. *Encyclopædia Inflationaris: Opiparous Edition*. *Phys. Dark Univ.* 5-6, 75–235. doi:[10.1016/j.dark.2024.101653](https://doi.org/10.1016/j.dark.2024.101653), [arXiv:1303.3787](https://arxiv.org/abs/1303.3787).
- McAllister, L., Silverstein, E., Westphal, A., 2010. Gravity Waves and Linear Inflation from Axion Monodromy. *Phys. Rev. D* 82, 046003. doi:[10.1103/PhysRevD.82.046003](https://doi.org/10.1103/PhysRevD.82.046003), [arXiv:0808.0706](https://arxiv.org/abs/0808.0706).
- Mukhanov, V.F., Chibisov, G.V., 1981. Quantum Fluctuations and a Nonsingular Universe. *JETP Lett.* 33, 532–535.
- Nelson, W., 2007. The Probability of inflation in Loop Quantum Cosmology. *PoS QG-Ph*, 029. doi:[10.22323/1.043.0029](https://doi.org/10.22323/1.043.0029), [arXiv:0708.3288](https://arxiv.org/abs/0708.3288).
- Parvizi, F., Heydari, S., Solbi, M., Karami, K., 2026. Loop quantum inflation with inverse volume corrections in light of ACT data. *JHEAp* 52, 100563. doi:[10.1016/j.jheap.2026.100563](https://doi.org/10.1016/j.jheap.2026.100563), [arXiv:2510.03882](https://arxiv.org/abs/2510.03882).
- Perez, A., 2013. The Spin Foam Approach to Quantum Gravity. *Living Rev. Rel.* 16, 3. doi:[10.12942/lrr-2013-3](https://doi.org/10.12942/lrr-2013-3), [arXiv:1205.2019](https://arxiv.org/abs/1205.2019).
- Polchinski, J., 2007. *String theory. Vol. 2: Superstring theory and beyond*. Cambridge Monographs on Mathematical Physics, Cambridge University Press. doi:[10.1017/CB09780511618123](https://doi.org/10.1017/CB09780511618123).
- Rovelli, C., 2004. *Quantum gravity*. Cambridge Monographs on Mathematical Physics, Univ. Pr., Cambridge, UK. doi:[10.1017/CB09780511755804](https://doi.org/10.1017/CB09780511755804).
- Rovelli, C., Smolin, L., 1988. Knot Theory and Quantum Gravity. *Phys. Rev. Lett.* 61, 1155. doi:[10.1103/PhysRevLett.61.1155](https://doi.org/10.1103/PhysRevLett.61.1155).
- Rovelli, C., Smolin, L., 1990. Loop Space Representation of Quantum General Relativity. *Nucl. Phys. B* 331, 80–152. doi:[10.1016/0550-3213\(90\)90019-A](https://doi.org/10.1016/0550-3213(90)90019-A).

- Schiffrin, J.S., Wald, R.M., 2012. Measure and Probability in Cosmology. *Phys. Rev. D* 86, 023521. doi:[10.1103/PhysRevD.86.023521](https://doi.org/10.1103/PhysRevD.86.023521), [arXiv:1202.1818](https://arxiv.org/abs/1202.1818).
- Silverstein, E., Westphal, A., 2008. Monodromy in the CMB: Gravity Waves and String Inflation. *Phys. Rev. D* 78, 106003. doi:[10.1103/PhysRevD.78.106003](https://doi.org/10.1103/PhysRevD.78.106003), [arXiv:0803.3085](https://arxiv.org/abs/0803.3085).
- Starobinsky, A.A., 1980. A New Type of Isotropic Cosmological Models Without Singularity. *Phys. Lett.* 91B, 99–102. [*Adv. Ser. Astrophys. Cosmol.*3,130(1987); ,771(1980)].
- Thiemann, T., 2007. *Modern Canonical Quantum General Relativity*. Cambridge Monographs on Mathematical Physics, Cambridge University Press. doi:[10.1017/CB09780511755682](https://doi.org/10.1017/CB09780511755682).
- Vereshchagin, G., Bedić, S., 2018. Loop Quantum Cosmology and Probability of Inflation. *Astron. Rep.* 62, 959–964. doi:[10.1134/S1063772918120326](https://doi.org/10.1134/S1063772918120326).
- Yuennan, J., Koad, P., Atamurotov, F., Channaie, P., 2025. Quantum-corrected ϕ^4 inflation in light of ACT observations. *Eur. Phys. J. C* 85, 1307. doi:[10.1140/epjc/s10052-025-15060-6](https://doi.org/10.1140/epjc/s10052-025-15060-6), [arXiv:2508.17263](https://arxiv.org/abs/2508.17263).